

*Short title: LARGE-SCALE MAGNETIC FIELD INSTABILITY*

# Dynamo effect in parity-invariant flow with large and moderate separation of scales

V.A. Zheligovsky<sup>a,b,c,1</sup>, O.M. Podvigina<sup>a,b,c,2</sup>, U. Frisch<sup>a,3</sup>

<sup>a</sup>Observatoire de la Côte d'Azur, CNRS UMR 6529,  
BP 4229, 06304 Nice Cedex 4, France

<sup>b</sup>International Institute of Earthquake Prediction Theory  
and Mathematical Geophysics,  
79 bldg. 2, Warshavskoe ave., 113556 Moscow, Russian Federation

<sup>c</sup>Laboratory of general aerodynamics, Institute of Mechanics,  
Lomonosov Moscow State University,  
1, Michurinsky ave., 119899 Moscow, Russian Federation

*Submitted to Geophysical Astrophysical Fluid Dynamics 1 December 2000*

## Abstract

It is shown that non-helical (more precisely, parity-invariant) flows capable of sustaining a large-scale dynamo by the negative magnetic eddy diffusivity effect are quite common. This conclusion is based on numerical examination of a large number of randomly selected flows. Few outliers with strongly negative eddy diffusivities are also found, and they are interpreted in terms of the closeness of the control parameter to a critical value for generation of a small-scale magnetic field. Furthermore, it is shown that, for parity-invariant flows, a moderate separation of scales between the basic flow and the magnetic field often significantly reduces the critical magnetic Reynolds number for the onset of dynamo action.

**Key words:** Eddy diffusivity, kinematic magnetic dynamo, multiscale expansion, instability.

---

<sup>1</sup>E-mail: vlad@mitp.ru

<sup>2</sup>E-mail: olgap@mitp.ru

<sup>3</sup>E-mail: uriel@obs-nice.fr

# 1 Introduction

The kinematic dynamo effect is generally believed to be facilitated by a separation of spatial scales between the flow and the magnetic field. This idea has its roots in the discovery of the  $\alpha$ -effect (Steenbeck *et al.*, 1966; Krause and Rädler, 1980) for non-parity-invariant flows (an instance of which are helical flows). Indeed, recent results indicate that helicity and scale separation can lead to experimental dynamos (Gailitis *et al.*, 2000; Busse, 2000, Stieglitz and Müller, 2000).

Lanotte *et al.* (1999) showed that scale separation can also be useful for flows possessing parity invariance and thus lacking  $\alpha$ -effect. They found a first instance of a three-dimensional parity-invariant flow, the “modified Taylor–Green flow”, which can amplify a large-scale magnetic field by a negative eddy diffusivity mechanism (Roberts, 1972; Kraichnan, 1976). Emergence of the  $\alpha$ -effect and the negative eddy diffusivity effect can be demonstrated by asymptotic theory involving, in principle, very large scale separation. Both the aforementioned experiments and numerical simulations with helical (Galanti *et al.*, 1992) or non-helical (Nore *et al.*, 1997) flows indicate that even a moderate scale separation of a factor two can help for obtaining a dynamo.

The following argument due to Fauve (1999) shows, how crucial for experimental dynamos it is to lower the critical magnetic Reynolds number  $R_m = LV/\eta$ . Here,  $L$  is the overall scale of the apparatus,  $V$  is the typical velocity and  $\eta$  is the (molecular) magnetic diffusivity. Given the typically very small value of the magnetic Prandtl number, the flow is expected to be strongly turbulent. Hence, the kinetic energy dissipated per unit time in the apparatus is  $P \sim \rho \ell^2 V^3$ , where  $\rho$  is the fluid density and  $\ell$  is the typical spatial scale of the velocity. Thus,  $P \sim \eta^{-1} \epsilon^{-2/3} (PL/\rho)^{1/3}$ , where  $\epsilon = \ell/L$  is the scale-separation factor. Therefore, the required pump power behaves as the cube of the attainable  $R_m$ . Since it is generally believed that the cost of an experiment scales roughly as its volume, i.e.  $\sim L^3$ , the cost scales as the ninth power of the attainable  $R_m$ . This makes it desirable to design apparatus with the lowest possible critical magnetic Reynolds number.

Our intention is to begin a systematic investigation of the kinematic dynamo effect for parity-invariant flows with large or moderate scale separation with emphasis on lowering the critical magnetic Reynolds number. Note, that parity-invariant flows are at least as “natural” as helical ones. Indeed, the

Navier-Stokes equations are parity-invariant. Hence, even if this particular symmetry, like most other symmetries, is broken by the mechanisms generating the flow, we can expect the symmetry to be dynamically restored in a statistical sense at high Reynolds numbers (Frisch, 1995). We shall work here with time-independent flows, which we may think of as being averages of turbulent flows. We are of course aware that time dependence of the flow may result in new effects in dynamo action; we leave this issue for future work.

The paper is organized as follows.

In Sections 2 and 3 we consider the case where the spatial scale of magnetic field is much larger than that of the flow. Then  $\epsilon$  is a natural small parameter, enabling one to apply asymptotic methods. Multiscale expansions in hydrodynamics may be viewed as adaptations of general homogenization methods used to determine effective large-scale transport coefficients of periodic or random materials (Bensoussan *et al.*, 1978; Kozlov, 1978; Zhikov *et al.*, 1979). Usually the effective coefficients cannot be obtained without solving suitable auxiliary small-scale problems. In three space dimensions this may require significant computational resources. In Lanotte *et al.* (1999) equations for the large-scale component of magnetic fields are derived by along the same lines as in previous works on negative eddy viscosity in ordinary incompressible hydrodynamics (Dubrulle and Frisch, 1991; Gama *et al.*, 1994; Wirth *et al.*, 1995). Here we use a similar but a distinct approach based on the work of Vishik (1986, 1987), which yields a complete decomposition of magnetic modes and their eigenvalues (in Appendix A arbitrarily high-order terms of such expansions are derived).

To investigate, how commonly the phenomenon of negative magnetic eddy diffusivity is exhibited by three-dimensional flows, we follow in Section 3 a strategy similar to the one, which Gama *et al.* (1994) applied to estimate the abundance of two-dimensional flows with negative eddy viscosity. By solving numerically the relevant auxiliary problems we determine the minimum over directions of the (anisotropic) magnetic eddy diffusivities for two ensembles of flows with random Fourier components. This way we determine the fraction of flows such that, when decreasing molecular magnetic diffusivity, a large-scale negative eddy diffusivity instability appears before the flow becomes a small-scale dynamo. An interpretation of “outliers” with strongly negative eddy diffusivity, found in computations, is given in Appendix B. Since it is important for our purpose to analyze as many instances as possible, we

have used a new efficient algorithm for solving the elliptic auxiliary problems arising from the two-scale expansion. This method is an outgrowth of the Chebyshev iterative method developed by Podvigina and Zheligovsky (1997) for self-adjoint negative definite linear operators. The operators arising in hydrodynamical problems are not self-adjoint, but they naturally split into a dominant self-adjoint negative definite part (the molecular diffusion term) and the remaining transport term. We can then combine Chebyshev methods with operator splitting to reduce the harm stemming from complex eigenvalues. This methods and its theoretical foundations are presented in detail in Zheligovsky (2001), available only in Russian. For the reader's convenience, the essentials are given in Appendix C.

In Section 4 we turn to cases with moderate scale separation (i.e. when  $\epsilon$  is finite). First, we consider instances of flows for which we already know that there is a negative magnetic eddy diffusivity, and we determine windows in  $\epsilon$  over which dynamo action is present. Second, we examine the case  $\epsilon = 1/2$ , that is, we assume that the magnetic field has a spatial period twice that of the flow, and study how the critical magnetic Reynolds number  $R_m$  is affected, compared to the case with no scale separation ( $\epsilon = 1$ ). In both types of computations we exploit the fact that, for space-periodic boundary conditions, eigenmodes have the form

$$\mathbf{H} = e^{i\epsilon \mathbf{q} \cdot \mathbf{x}} \mathbf{h}(\mathbf{x}; \epsilon, \mathbf{q}), \quad (1)$$

where  $\mathbf{q}$  is a prescribed wavevector. This enables one to solve a problem involving only small scales, but parameterized by  $\epsilon$  and  $\mathbf{q}$  (cf. Roberts, 1972; Frisch *et al.*, 1986). Solution of the eigenvalue problem is more CPU-intensive than the solution of auxiliary problems involved in the asymptotic case (because efficient preconditioning techniques are available for the latter). Numerical methods and codes used for the eigenvalue computations are adapted from Zheligovsky (1993).

In Section 5 we summarize our main results.

## 2 Asymptotic expansion of magnetic modes and of their eigenvalues

Here we briefly review the asymptotic expansion arising in the kinematic dynamo problem, when the scale ratio  $\epsilon$  is small. The conducting fluid flow

$\mathbf{v}(\mathbf{x})$  is assumed to be time-independent, and the problem therefore reduces to the eigenvalue problem for the magnetic induction operator

$$\eta \nabla^2 \mathbf{H} + \nabla \times (\mathbf{v} \times \mathbf{H}) = \lambda \mathbf{H} \quad (2)$$

in the space of solenoidal vector fields:

$$\nabla \cdot \mathbf{H} = 0. \quad (3)$$

Here  $\eta > 0$  is magnetic molecular diffusivity,  $\mathbf{H}(\mathbf{x})$  is a magnetic mode and  $\lambda$  is the associated eigenvalue (the real part of which is here referred to as the growth rate of the mode; negative growth rates correspond to decaying modes). The flow is assumed incompressible:

$$\nabla \cdot \mathbf{v} = 0, \quad (4)$$

$2\pi$ -periodic in space and parity-invariant:

$$\mathbf{v}(\mathbf{x}) = -\mathbf{v}(-\mathbf{x}). \quad (5)$$

The magnetic mode  $\mathbf{H}(\mathbf{x}, \mathbf{y})$  is supposed to depend on the fast variable  $\mathbf{x}$  and on the slow variable  $\mathbf{y} = \epsilon \mathbf{x}$ , and is  $2\pi$ -periodic in both fast and slow variables (the velocity  $\mathbf{v}$  is independent of slow variables). Introduction of the two spatial scales results in a “decomposition of the gradient”  $\nabla \rightarrow \nabla_{\mathbf{x}} + \epsilon \nabla_{\mathbf{y}}$  in (2) and (3). Here and in what follows the subscripts  $\mathbf{x}$  and  $\mathbf{y}$  refer to differential operators in fast and slow variables, respectively.

Let  $\langle \cdot \rangle$  and  $\{ \cdot \}$  denote the mean (over the periodicity cube) and the fluctuating part of a vector field, respectively:

$$\langle \mathbf{f} \rangle = (2\pi)^{-3} \int_{T^3} \mathbf{f}(\mathbf{x}, \mathbf{y}) d\mathbf{x}, \quad \{ \mathbf{f} \} = \mathbf{f} - \langle \mathbf{f} \rangle. \quad (6)$$

Parity invariance (5) implies  $\langle \mathbf{v} \rangle = 0$ .

Solutions to the eigenproblem (2)-(5) are sought in the form of asymptotic series

$$\mathbf{H} = \sum_{n=0}^{\infty} \mathbf{h}_n(\mathbf{x}, \mathbf{y}) \epsilon^n, \quad (7)$$

$$\lambda = \sum_{n=0}^{\infty} \lambda_n \epsilon^n. \quad (8)$$

As shown in Appendix A, substitution of these expansions in (2) leads to a hierarchy of equations. By application of standard techniques for singular perturbation expansions, terms in the expansion eigenvalues are successively determined from solvability conditions, obtained here by just averaging the equations. In particular, it can be shown that  $\lambda_0 = \lambda_1 = 0$ , and the leading term  $\lambda_2$  in the series (8) can be determined from the following eigenvalue problem

$$\eta \nabla_{\mathbf{y}}^2 \langle \mathbf{h}_0 \rangle + \nabla_{\mathbf{y}} \times \sum_{k=1}^3 \sum_{m=1}^3 \mathbf{D}_{mk} \frac{\partial \langle h_0^k \rangle}{\partial y_m} = \lambda_2 \langle \mathbf{h}_0 \rangle, \quad (9)$$

subject to the solenoidality condition

$$\nabla_{\mathbf{y}} \cdot \langle \mathbf{h}_0 \rangle = 0. \quad (10)$$

Thus, the leading terms of the expansions in powers of  $\epsilon$  of the mean magnetic field and of the eigenvalue turn out to be, respectively, an eigenfunction and the associated eigenvalue of a partial differential operator comprised only of second order derivatives, which may be regarded as representing an anisotropic diffusion. However, this operator is not necessarily dissipative: it may have eigenvalues with positive real parts. In this context one then may speak of negative eddy diffusivity.

The coefficients  $\mathbf{D}_{mk}$  of this partial differential operator can be expressed in terms of solutions of a set of auxiliary problems:

$$\eta \nabla^2 \mathbf{S}_k + \nabla \times (\mathbf{v} \times \mathbf{S}_k) = -\frac{\partial \mathbf{v}}{\partial x_k} \quad (11)$$

and

$$\eta \nabla^2 \mathbf{\Gamma}_{mk} + \nabla \times (\mathbf{v} \times \mathbf{\Gamma}_{mk}) = -2\eta \frac{\partial \mathbf{S}_k}{\partial x_m} + v^m (\mathbf{S}_k + \mathbf{e}_k) - \mathbf{v} S_k^m, \quad (12)$$

which will be referred to as the first and the second auxiliary problem, respectively. Here,  $\mathbf{e}_k$  is the unit vector in the  $k$ -th cartesian coordinate direction and superscripts denote cartesian components of vectors. For solutions to (11) and (12) to exist, we require that zero should not be an eigenvalue of the magnetic induction operator

$$\mathcal{L}\mathbf{H} \equiv \eta \nabla^2 \mathbf{H} + \nabla \times (\mathbf{v} \times \mathbf{H}),$$

restricted to small-scale solenoidal vector fields with the vanishing mean; by “small-scale” we mean independent of the slow variable. Generically this condition is satisfied. It is then found that

$$\mathbf{D}_{mk} = \langle \mathbf{v} \times \mathbf{\Gamma}_{mk} \rangle. \quad (13)$$

Problems (11) and (12) are formulated with a  $2\pi$ -periodicity boundary condition for the vector fields  $\mathbf{S}_k(\mathbf{x})$  and  $\mathbf{\Gamma}_{mk}(\mathbf{x})$ , which should also have a vanishing mean. It follows that the  $\mathbf{S}_k$ ’s are parity-antiinvariant ( $\mathbf{S}_k(\mathbf{x}) = \mathbf{S}_k(-\mathbf{x})$ ) and solenoidal ( $\nabla \cdot \mathbf{S}_k = 0$ ), and that the  $\mathbf{\Gamma}_{mk}$ ’s are parity-invariant ( $\mathbf{\Gamma}_{mk}(\mathbf{x}) = -\mathbf{\Gamma}_{mk}(-\mathbf{x})$ ).

Since the homogenized operator defined by (9)-(10) has constant coefficients, its eigenvectors are Fourier harmonics:  $\langle \mathbf{h}_0 \rangle = \mathbf{h} e^{i\mathbf{q} \cdot \mathbf{y}}$ , where  $\mathbf{h}$  and  $\mathbf{q}$  are constant vectors. The wavevector  $\mathbf{q}$  is taken real because we are only interested in modes uniformly bounded in the entire space. Substitution in (9)-(10) yields

$$\eta |\mathbf{q}|^2 \mathbf{h} + \mathbf{q} \times \sum_{k=1}^3 \sum_{m=1}^3 \mathbf{D}_{mk} h^k q^m = -\lambda_2 \mathbf{h}, \quad (14)$$

$$\mathbf{h} \cdot \mathbf{q} = 0. \quad (15)$$

### 3 Abundance of flows producing negative magnetic eddy diffusivity

Following Gama *et al.* (1994), we now ask how common is the phenomenon of negative diffusivity.

Time-independent periodic flows, satisfying (4)-(5), are represented here by their Fourier series

$$\mathbf{v} = \sum_{|\mathbf{k}|=1}^N \mathbf{v}_{\mathbf{k}} e^{i\mathbf{k} \cdot \mathbf{x}} \quad (16)$$

with random amplitude harmonics. For the velocity to be real,  $\mathbf{v}_{\mathbf{k}} = \overline{\mathbf{v}_{-\mathbf{k}}}$ , and parity invariance (5) requires  $\text{Re } \mathbf{v}_{\mathbf{k}} = 0$ .

We study two ensembles of flows with different types of fall-offs of the energy spectrum  $E_K$ . The latter is defined as the total energy contained in harmonics, whose wavevectors  $\mathbf{k}$  belong to the  $K$ -th spherical shell, i.e.

Table 1. Statistics of the eddy diffusivities for the considered ensembles of flows.

	Exponential spectrum flows			Hyperbolic spectrum flows		
	$\eta = 0.3$	$\eta = 0.2$	$\eta = 0.1$	$\eta = 0.3$	$\eta = 0.2$	$\eta = 0.1$
$\text{Re } \eta_{\text{eddy}} < 0$	0%	18%	86%	0%	4%	53%
$\text{Re } \eta_{\text{eddy}} < \eta$	83%	96%	98%	30%	63%	94%
complex $\eta_{\text{eddy}}$	7%	2%	2%	8%	5%	3%

$K - 1 < |\mathbf{k}| \leq K$ , where  $K > 0$  is integer. When  $E_K \propto e^{-\xi K}$ , the flow is said to have exponential spectrum; when  $E_K \propto K^{-1}$ , it is said to have hyperbolic spectrum. These have respectively rapid and slow fall-offs. The spectra are band-limited and set to zero beyond wavenumber  $N = 10$  for the exponential case and beyond  $N = 7$  for the hyperbolic case. The value  $\xi = 10^{-2/3}$  is used throughout in the exponential case.

The flows are produced by the following procedure (applied only to one half of the set of wavevectors, the second one being related by complex conjugation). For  $\mathbf{k}$  in the ball  $1 \leq |\mathbf{k}| \leq N$ , random imaginary vectors  $\mathbf{r}_{\mathbf{k}}$  are generated with the imaginary part of each cartesian component uniformly distributed in the interval  $[-0.5, 0.5]$  (the RAN2 random number generator by Press *et al.*, 1992, is used). Then the vectors  $\mathbf{r}_{\mathbf{k}}$  are projected onto the plane perpendicular to  $\mathbf{k}$  to gain incompressibility. Finally, the obtained vectors are normalized, so that the flow has the desired energy spectrum and the root-mean-square velocity is one, when the normalized vectors are employed as the Fourier coefficients  $\mathbf{v}_{\mathbf{k}}$  in (16).

Each ensemble consists of 100 flows. For each flow, computations are carried out for three values of molecular diffusivity,  $\eta = 0.3$ ,  $0.2$  and  $0.1$ . All computations are performed with the resolution of  $64^3$  Fourier harmonics, employing standard spectral methods based on fast Fourier transforms and dealiasing. (Each case requires from 10 to 30 minutes of CPU on one DEC Alpha EV6 processor, depending on the value of  $\eta$ .) The power spectra of the solutions to (11) and (12) turn out to decrease monotonically very quickly for  $K \geq 2$ . For  $\eta = 0.1$  in the hyperbolic case (resp. exponential case), the decrease is typically by 7-8 orders of magnitude (14-15 orders of magnitude) from maximum to minimum.

After the homogenized coefficients (13) are determined, the minimum



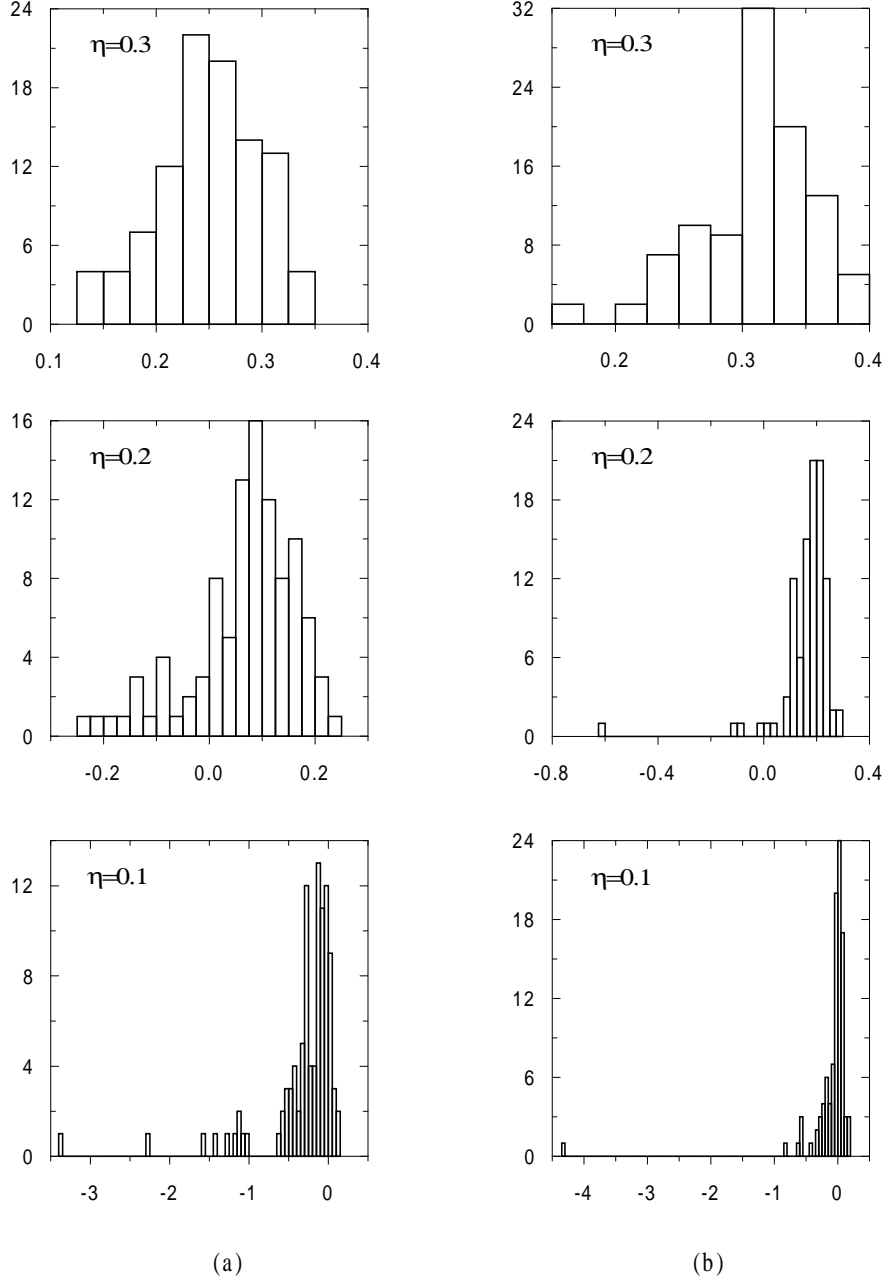


Figure 1: Histograms of the minimum eddy diffusivity values  $\eta_{\text{eddy}}$  (horizontal axis) for ensembles of 100 parity-invariant flows with exponential (a) and hyperbolic (b) spectra.

magnetic eddy diffusivity

$$\eta_{\text{eddy}} = \min_{|\mathbf{q}|=1} (-\lambda_2(\mathbf{q}))$$

is calculated as the minimum eigenvalue of the problem (14)-(15). (Note, that with a unit wavevector the eigenvalue is just the opposite of the eddy diffusivity.) For a given  $\mathbf{q}$  this eigenproblem yields two eigenvalues satisfying a quadratic equation; the eigenvalues can thus be complex conjugate (a similar phenomenon was observed for three-dimensional eddy viscosities; see Wirth *et al.*, 1995). Then the minimum of the real part of the complex eddy diffusivity, which determines the maximum rate of instability of a large-scale magnetic perturbation, is sought. However, in our computations complex eddy diffusivities appear quite rarely (see Table 1).

Histograms of the obtained magnetic eddy diffusivities are shown on Figure 1. The statistics of eddy diffusivities shown in Table 1 indicate that flows with the exponential energy spectrum are more efficient in lowering the minimum of the eddy diffusivity than those with the hyperbolic spectrum. This suggests that low wavenumber harmonics of the underlying flow are more important for lowering than high wavenumber harmonics.

We note that our code reproduces the negative eddy diffusivity values obtained by an alternative numerical method by Lanotte *et al.* (1999) for the modified Taylor–Green flow.

A physically important question is: which instability arises first, when magnetic molecular diffusivity is decreased, a large-scale or a small-scale one? Similarly to what was done by Gama *et al.* (1994), for each considered pair of a flow and a molecular diffusivity it is checked that small-scale magnetic fields with a vanishing mean are stable, i.e. have negative growth rate (see Figures 2 and 3).

Several “outliers” with relatively large negative eddy diffusivities can be seen on the histograms shown on Figure 1 for  $\eta = 0.1$ . This can be explained as follows. We see on Figures 2 and 3 that in the case of outliers the growth rate of *small-scale* magnetic modes (plotted horizontally) is negative, but close to zero. Furthermore, we have checked that the corresponding eigenvalue is real. In other words, we are close to a non-oscillatory small-scale instability threshold. Now, we observe that the expression of the eddy diffusivity, derived in Section 2 and Appendix A, involves the inverse of the small-scale magnetic induction operator. It is thus not surprising that large

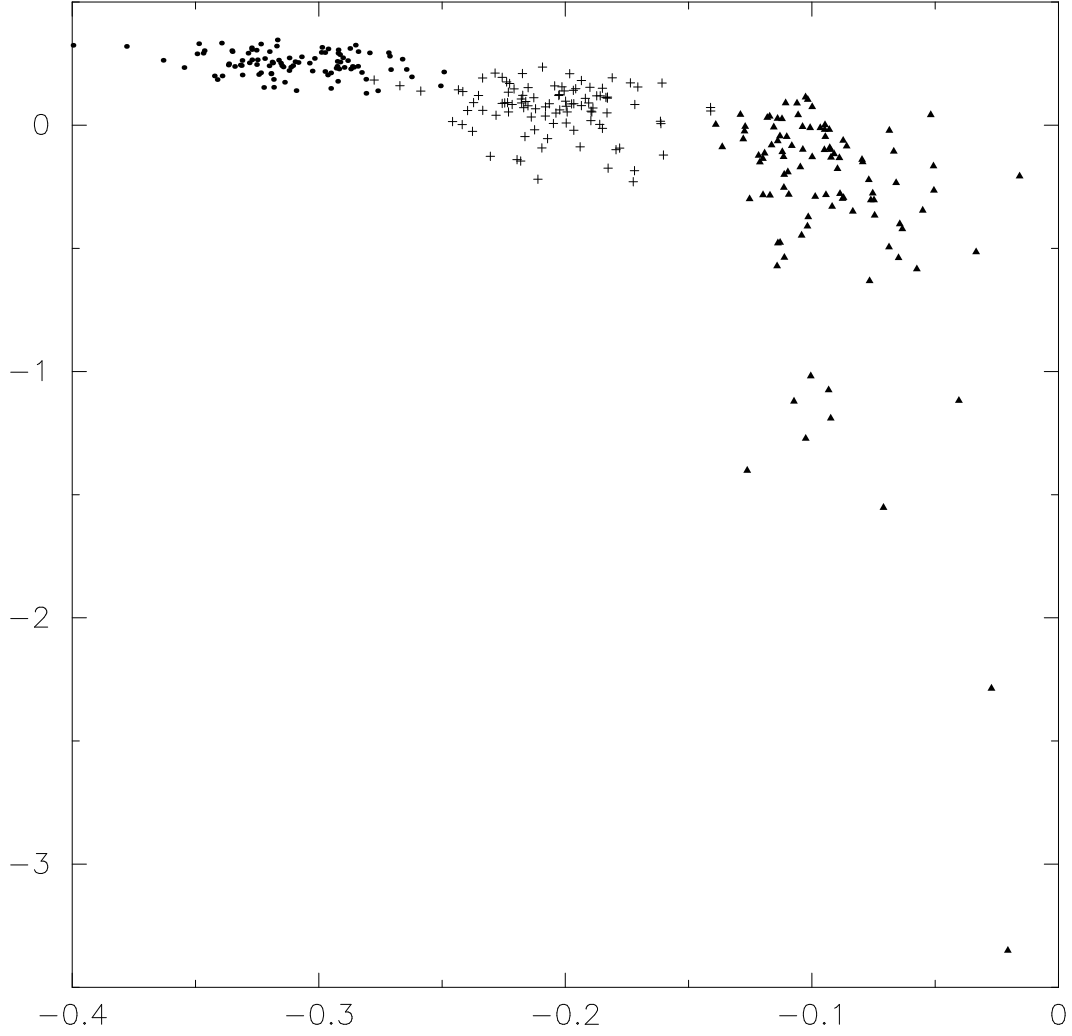


Figure 2: Minimum eddy diffusivity  $\eta_{\text{eddy}}$  (vertical axis) versus the growth rate of the corresponding dominant small-scale magnetic modes (horizontal axis) for  $\eta = 0.3$  (dots),  $0.2$  (pluses) and  $0.1$  (triangles) and 100 different flows with the exponential spectrum.

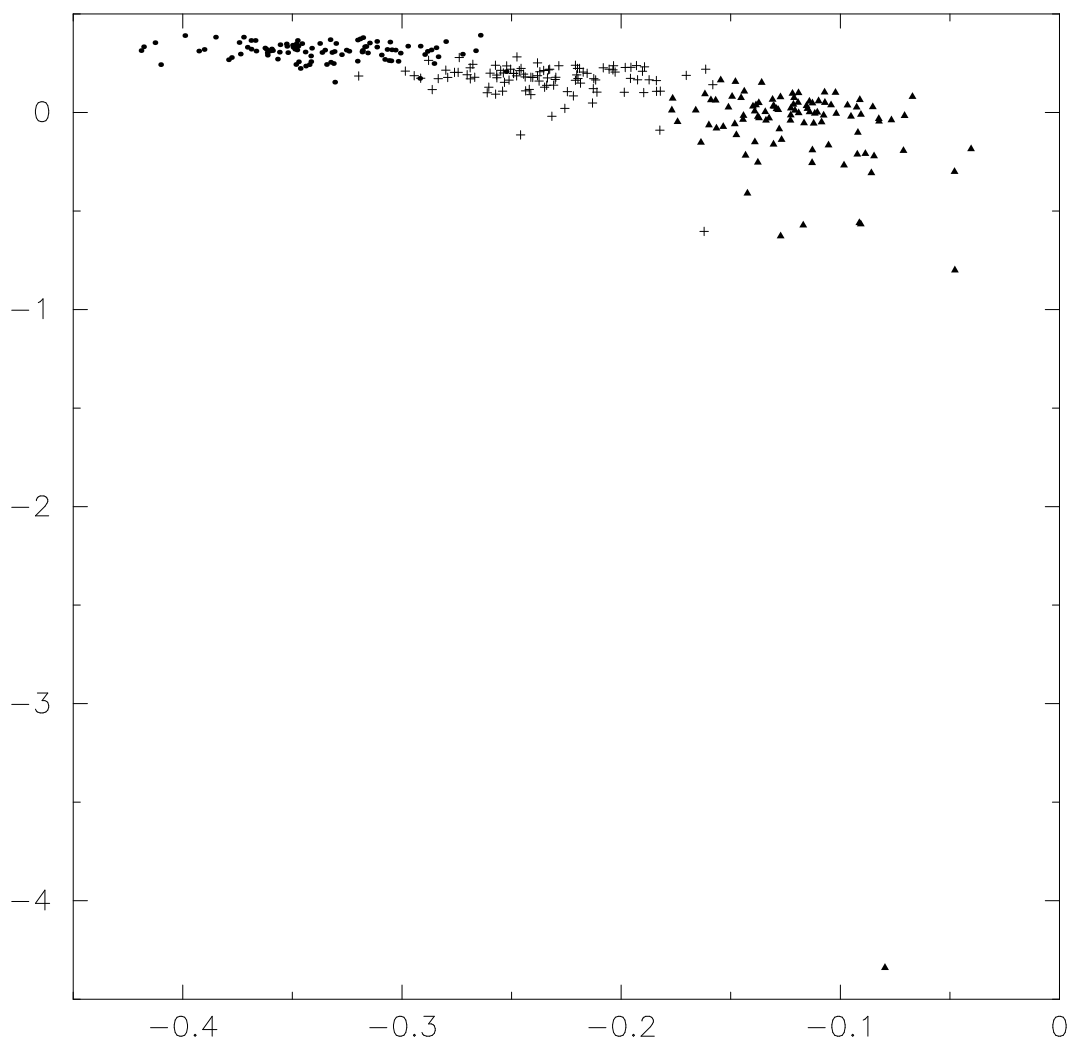


Figure 3: Same as Figure 2 but with the hyperbolic spectrum.

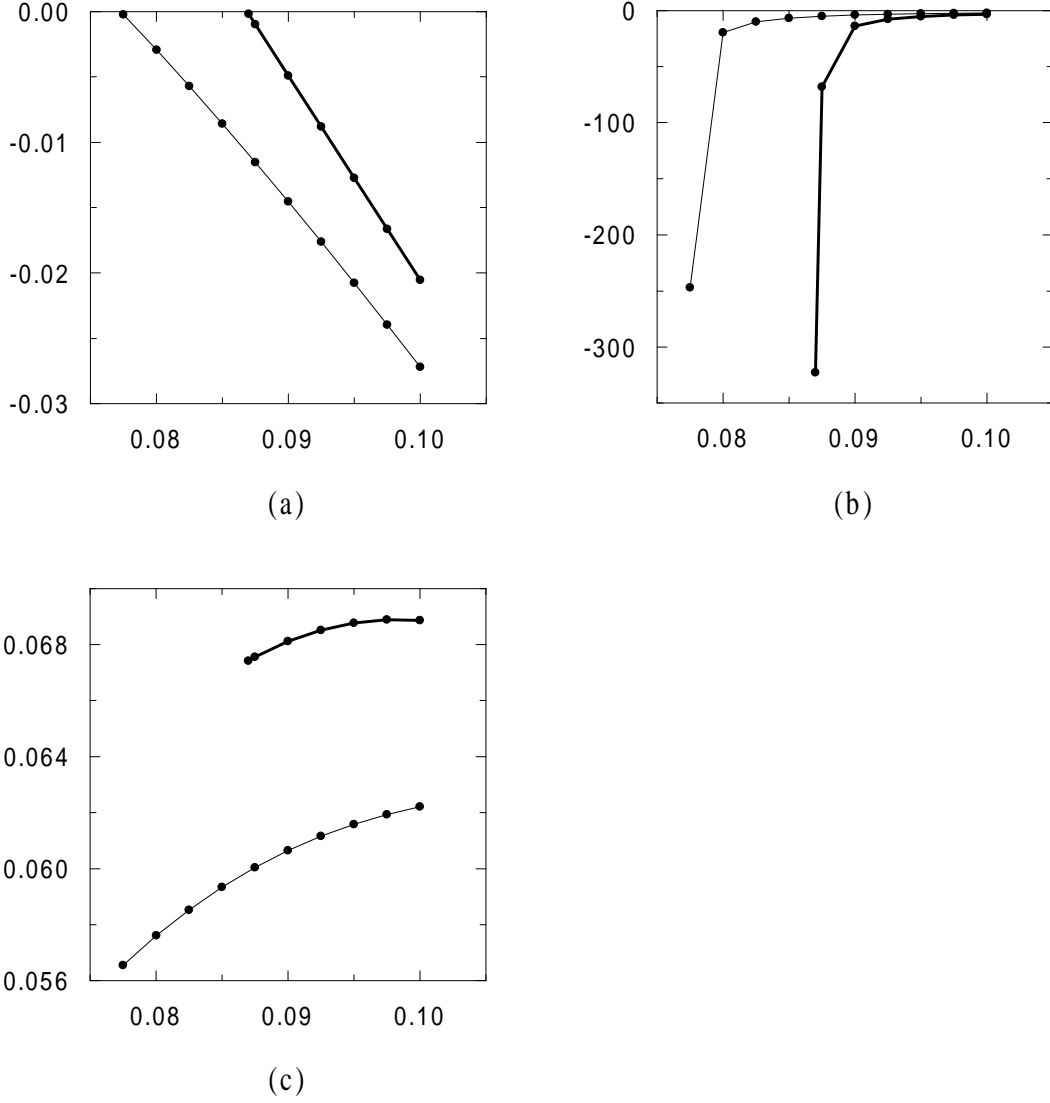


Figure 4: Maximum growth rates  $\zeta_1$  of small-scale magnetic modes (a), minimum magnetic eddy diffusivity  $\eta_{\text{eddy}}$  (b) and product  $\zeta_1 \eta_{\text{eddy}}$  (c) all plotted versus molecular diffusivity  $\eta$ . Line width codes two flow realizations, corresponding to the two right-lower corner outliers in Figure 2.

eddy diffusivities can be obtained. Depending on whether a certain inequality is satisfied at the threshold, this eddy diffusivity can be either large negative or large positive (see details in Appendix B). We have checked numerically that the outlier eddy diffusivities are approximately inversely proportional to the small dominant eigenvalue (see Figure 4).

Note, that if we are exactly at the threshold, our two-scale expansion breaks down. A modified expansion can be carried out which takes into account the enlargement of the kernel of the magnetic induction operator  $\mathcal{L}$ . In the presence of a large-scale perturbation this can lead to an eigenvalue  $O(\epsilon)$  rather than the  $O(\epsilon^2)$ -dependence obtained in the general parity-invariant case. In other words, the large-scale dynamics can be governed by a first-order differential operator.

## 4 Generation of magnetic field with moderate scale separation

For intermediate values of  $\epsilon$ , corresponding to moderate scale separation, direct evaluation of the most unstable magnetic modes is desirable. Computations are simplified by the fact that eigenmodes have the form (1), all the dependence on the slow variable  $\mathbf{y} = \epsilon\mathbf{x}$  being absorbed into an exponential factor  $e^{i\epsilon\mathbf{q}\cdot\mathbf{x}}$ . Since the flow is assumed to depend only on the fast variable  $\mathbf{x}$ , the eigenvalue problem is reduced to a small-scale one for a *modified operator* by changing  $\nabla \rightarrow \nabla_{\mathbf{x}} + i\epsilon\mathbf{q}$  in the magnetic induction operator (2) and in the solenoidality condition (3).

To find the most unstable magnetic mode one must, in principle, allow for arbitrary orientations of the vector  $\mathbf{q}$ . Throughout this section we assume only “binary”  $\mathbf{q}$ ’s such that each component takes only the values 0 or 1, so that  $\epsilon^{-1}$  may be regarded as the maximum scale-separation factor over cartesian directions.

Since our simulations are computationally demanding, we choose for each flow only one  $\mathbf{q}$ -direction as follows. For a given flow and for the molecular diffusivity  $\eta = 0.1$ , we obtain the most unstable  $\mathbf{q}$ -directions *in the asymptotic regime*  $\epsilon \rightarrow 0$  from the results of Section 3. It turns out that for the cases reported in this section, these directions are approximately parallel to binary vectors with one or two non-zero components. These binary vectors are then

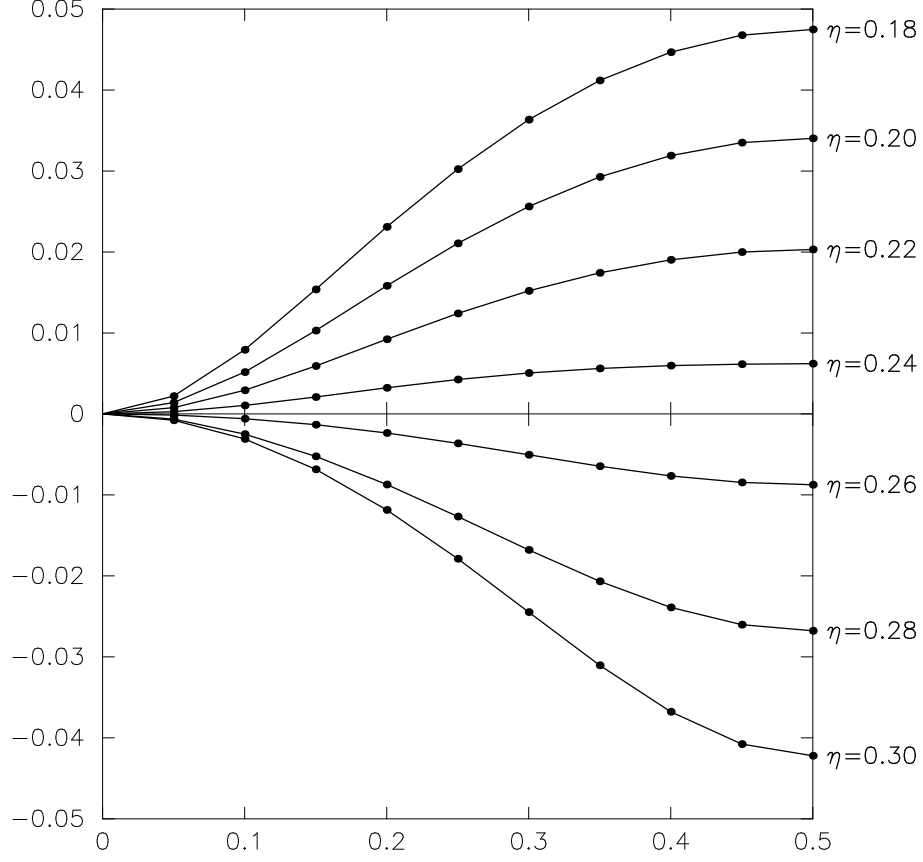


Figure 5: Maximum growth rates of magnetic modes (vertical axis) versus the scale ratio  $\epsilon$  (horizontal axis) for different molecular diffusivities  $\eta$  and one of four samples of a flow with the hyperbolic spectrum.

employed when  $\epsilon$  is finite for all values of  $\eta$  studied.

Figures 5-8 show the dominant growth rates for four different flows selected out of the ensemble of flows with hyperbolic spectrum, which sustain negative eddy diffusivity. Actually, when  $\mathbf{q}$  has integer components, it is only necessary to make computations for  $0 \leq \epsilon \leq 1/2$ . Indeed, first note, that the modified magnetic induction operators for two values of  $\epsilon$  differing by 1 have the same spectrum and their eigenfunctions differ by a factor  $e^{i\mathbf{q}\mathbf{x}}$ . Second, by parity invariance of the velocity (5), for two opposite values of  $\epsilon$  the spectra are also the same and eigenfunctions are related by parity  $\mathbf{H}(\mathbf{x}) \rightarrow \mathbf{H}(-\mathbf{x})$ .

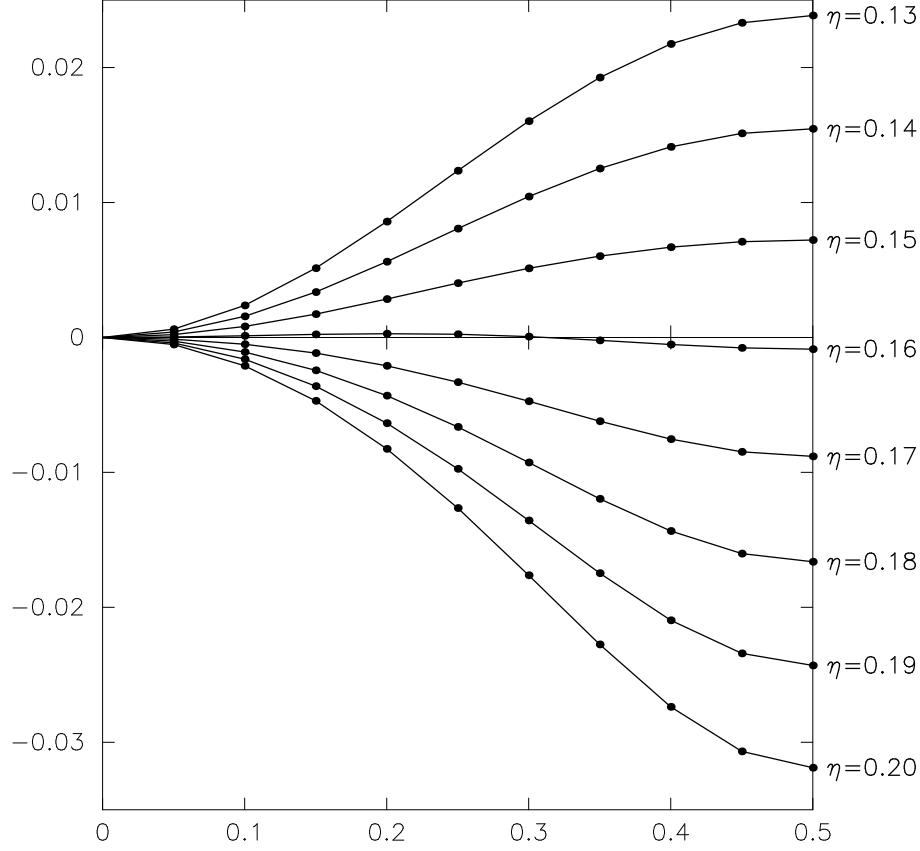


Figure 6: Same as Figure 5, another flow sample.

(From this one easily deduces that the spectrum of the modified operator is complex conjugate, eigenvalues  $\lambda$  and  $\bar{\lambda}$  being associated to eigenfunctions  $\mathbf{H}(\mathbf{x})$  and  $\bar{\mathbf{H}}(-\mathbf{x})$ , respectively.) Hence, outside the interval  $0 \leq \epsilon \leq 1/2$  the plots can be continued by symmetry about the vertical line  $\epsilon = 1/2$  and by 1-periodicity.

The results reported here are obtained with the resolution of  $64^3$  Fourier harmonics. For the “worst” case,  $\eta = 0.07$ , they differ only in the third significant digit from those obtained with the resolution  $32^3$ . Note, that energy spectra of the computed magnetic modes decrease by at least 4 orders of magnitude for  $\eta = 0.13$  and by at least 5 for  $\eta = 0.3$ , indicating that the employed resolution is adequate. (For  $\eta = 0.07$  the decrease is only by 3



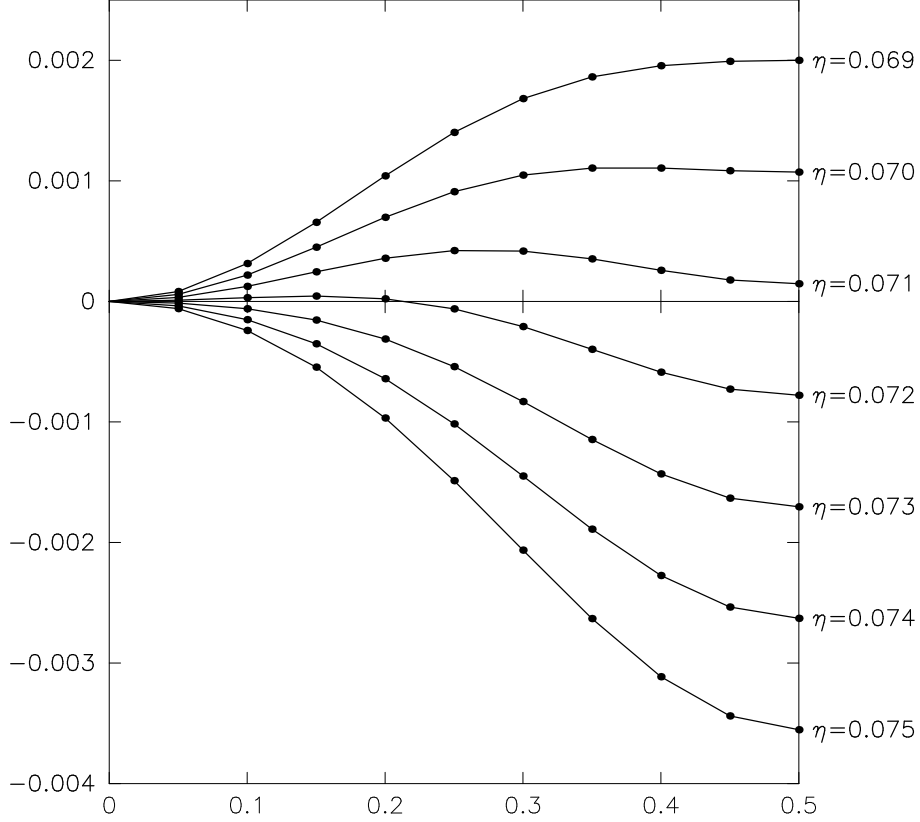


Figure 7: Same as Figure 5, yet another flow sample.

orders of magnitude, which may seem marginal. However, it is well-known that eigenvalues are less sensitive to insufficient resolution, than the fine structure of eigenmodes.)

Inspection of Figures 6-8 reveals that there can be one or more windows in scale separation, where the dynamo (positive growth rate) is present, whereas in Figures 5 the dynamo appears to be present for all scale separations, provided the eddy diffusivity is negative. In Figure 8 the two windows belong to two different analytical branches of eigenvalues and eigenmodes, with the transition occurring near  $\epsilon = 0.3$ .

Note, that all the growth rates vanish (quadratically) when  $\epsilon \rightarrow 0$ . The reason is that the small- $\epsilon$  eigenvalues, obtained by the two-scale expansion of Section 2, are analytic continuations of the zero eigenvalue in the small-

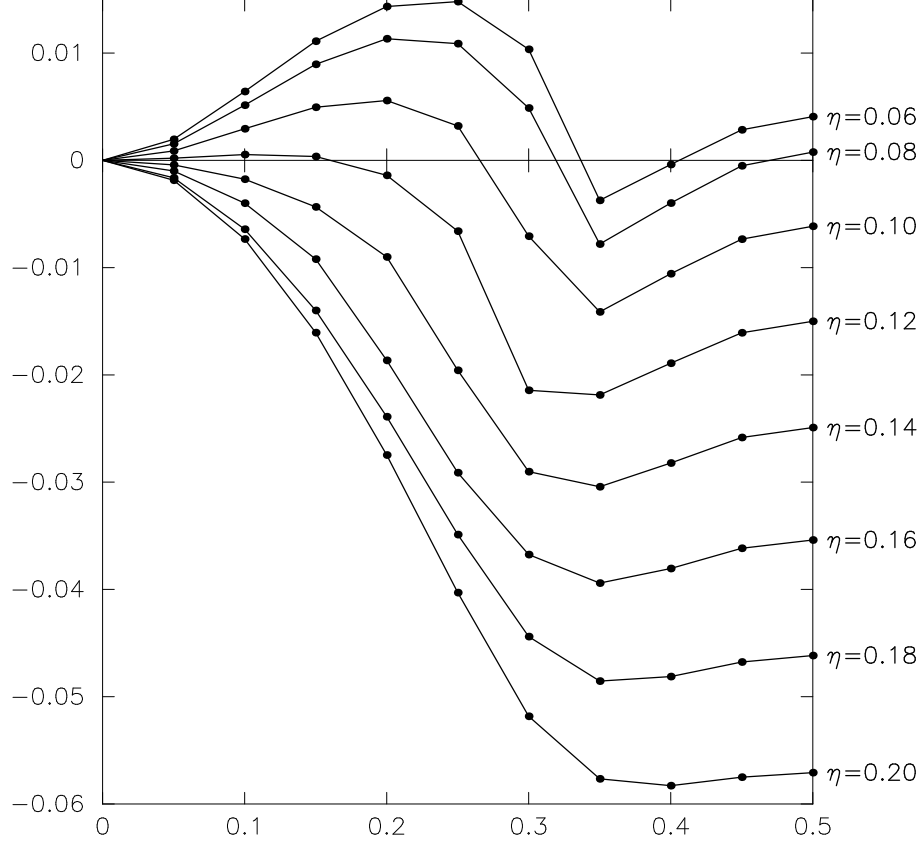


Figure 8: Same as Figure 5, the last flow sample.

scale problem. The presence of the eigenvalue zero is due to the structure of the magnetic induction operator, which is the curl of a first-order operator. (Hence, its adjoint, acting also in the space of divergenceless functions

$$\mathcal{L}^* : \mathbf{H} \mapsto \eta \nabla_{\mathbf{x}}^2 \mathbf{H} + (\nabla_{\mathbf{x}} \times \mathbf{H}) \times \mathbf{v} - \nabla_{\mathbf{x}} p$$

has constant vectors in its kernel.) Conversely, it can be demonstrated by spatial averaging of  $\mathcal{L}\mathbf{H} = \lambda\mathbf{H}$ , that for a mode with a non-vanishing mean the associated eigenvalue equals 0. (Note, that in Section 3 we restricted the operator to functions of vanishing spatial mean and thus the growth rate zero was absent from Figures 2 and 3.)

We now turn to the case, where there is a finite scale separation of a factor two ( $\epsilon = 1/2$ ). The question we address is: how does a mere doubling

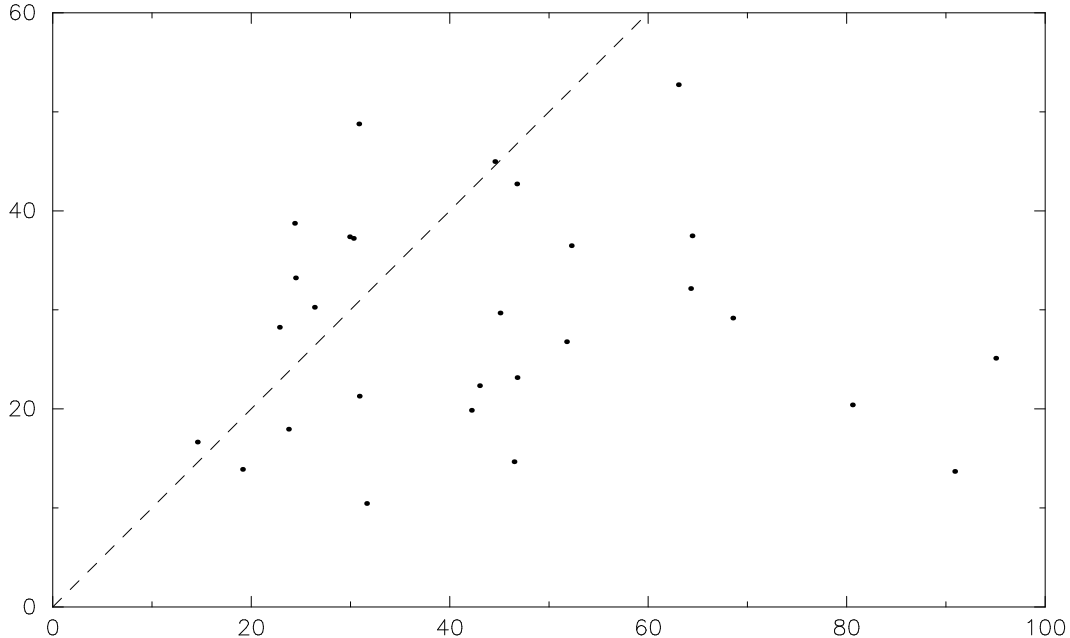


Figure 9: Critical magnetic Reynolds numbers for the onset of instability of small-scale magnetic modes (horizontal axis) versus critical magnetic Reynolds numbers for magnetic modes of twice the spatial period (vertical axis). 28 flows with the hyperbolic spectrum are shown. The dashed line corresponds to equal Reynolds numbers.

of the spatial period of magnetic modes (relative to that of the basic flow) affect generation? More precisely: to lower the critical magnetic Reynolds number, does it help to introduce such a scale separation? We systematically compare critical numbers when  $\epsilon = 1$  (no scale separation) and  $\epsilon = 1/2$  for an ensemble of flows with hyperbolic energy spectrum. We define our magnetic Reynolds numbers  $R_m = LV/\eta$  in terms of the *largest* scale available  $L = \epsilon^{-1}$  (the inverse of the minimum wavenumber of the magnetic field) and of the r.m.s. velocity  $V$ . In computations  $V = 1$  and hence  $R_m = (\epsilon\eta)^{-1}$ .

When  $\epsilon = 1/2$  we face again the problem, mentioned earlier, of choosing the vectors  $\mathbf{q}$ . For each flow we now search for the critical  $R_m$ , allowing all

7 possible binary  $\mathbf{q} \neq 0$ . More precisely, we find an approximate (minimum) critical  $R_m$  and the corresponding  $\mathbf{q}$  by running our code with  $32^3$  Fourier harmonics, and then refine the critical  $R_m$  with  $64^3$  Fourier harmonics for the obtained  $\mathbf{q}$ .

The secant method was used to find stationary modes. Iterations were terminated when the real part of the dominant eigenvalue was below  $10^{-5}$  in magnitude. This usually required 4-5 iterations.

As far as the accuracy of the calculation is concerned, note that in all  $\epsilon = 1/2$  runs with  $R_m > 25$  the energy spectrum decreases by at least 4 orders of magnitude, an indication that  $64^3$  harmonics provide sufficient resolution. In the most demanding runs, with  $\epsilon = 1$  and  $R_m > 50$ , the energy spectra decrease only by 2-3 orders of magnitude but, as pointed out before, eigenvalues are computed nevertheless quite accurately (critical  $R_m$ 's, computed with the  $32^3$  and  $64^3$  resolutions, differ in the third significant digit).

Figure 9 shows all the critical  $R_m$ 's calculated for 28 cases. Two cases not shown have critical  $R_m = 30.7$  and  $25.3$  when  $\epsilon = 1/2$ , but do not display dynamo action for any  $Rm \leq 100$  when  $\epsilon = 1$ . The results demonstrate that scale separation lowers the critical  $R_m$  in all but 9 cases out of the 30 studied.

## 5 Conclusion

Three main results are presented in this work.

First, in Section 3, we demonstrated that parity-invariant flows possessing a negative magnetic eddy diffusivity are quite common. Specifically, we generated two random ensembles of flows; both had time-independent randomly chosen Fourier components, one with an exponentially decreasing energy spectrum, the other – with a power-law decrease (referred to as “hyperbolic” because the exponent is -1). One hundred independent selections were made in each case and three different molecular magnetic diffusivities were used, all corresponding to small-scale magnetic Reynolds numbers not exceeding ten. None of the 600 cases investigated was a small-scale dynamo. For the lowest diffusivity considered, 86% of the “exponential” spectrum flows and 53% of the “hyperbolic” spectrum flows produced a negative eddy diffusivity and, hence, can act as a large-scale dynamo (for more details, see Table 1).

Second, several instances with particularly negative eddy diffusivities were encountered. The theory of these “outliers” (given in details in Appendix B) relates them to a near-critical state, where an eigenvalue of the small-scale dynamo problem is about to pass through zero (there is also an additional inequality ensuring that a large *negative* value is obtained).

Finally, we presented numerical evidence that, for a parity-invariant flow, even a moderate scale separation between the flow and the magnetic field is generally beneficial for magnetic field generation. Specifically, we showed that the critical magnetic Reynolds number based on the largest scale present (that of the magnetic field) is often lowered when the scale of twice the spatial period of the velocity is introduced (70% of the instances studied had this property; see Figure 9). For a few flows we also studied the dependence on the scale-separation factor, when it is varied from a 1:2 ratio to a 1:20 ratio. One instance (shown in Figure 8) has a window lacking dynamo action between low and large values, where it is present.

### **Acknowledgments.**

We are grateful to the authors of Lanotte *et al.* (1999) for making available to us the source of the code used to obtain the results reported in their paper and to S. Fauve, S. Gama, A. Lanotte, A. Noullez, Y. Ponty and M. Vergassola for useful discussions. Computational facilities were provided by the program “Simulations Interactives et Visualisation en Astronomie et Mécanique (SIVAM)” at the Observatoire de la Côte d’Azur. Visits of O.M. Podvigina and V.A. Zheligovsky were supported by the French Ministry of Education.

## Appendices

### A Formal asymptotic expansion of magnetic modes and the associated eigenvalues

We construct here complete asymptotic expansions of magnetic eigenmodes and of their eigenvalues for small values of the scale ratio  $\epsilon$ . Assumptions concerning the flow were listed in Section 2.

The kinematic dynamo problem reduces to the eigenvalue problem

$$\mathcal{M}\mathbf{H} = \lambda\mathbf{H}. \quad (\text{A.1})$$

Here  $\mathbf{H}(\mathbf{x})$  is a magnetic mode,  $\lambda$  is its eigenvalue, and

$$\mathcal{M}\mathbf{H} \equiv \eta\nabla^2\mathbf{H} + \nabla \times (\mathbf{v} \times \mathbf{H}),$$

acting in the space of solenoidal vector fields, is the magnetic induction operator (it acts like  $\mathcal{L}$ , but in a larger domain). The magnetic mode  $\mathbf{H}(\mathbf{x}, \mathbf{y})$  is supposed to be solenoidal (3) and  $2\pi$ -periodic in both fast and slow variables. Solutions to the eigenproblem (A.1) are sought in the form of asymptotic series  $\mathbf{H} = \sum \mathbf{h}_n \epsilon^n$  and  $\lambda = \sum \lambda_n \epsilon^n$ . Denote

$$\mathbf{H}_n \equiv \langle \mathbf{h}_n \rangle; \quad \mathbf{G}_n \equiv \{ \mathbf{h}_n \},$$

where  $\langle \cdot \rangle$  and  $\{ \cdot \}$  refer to the mean and fluctuating part (see (6)), respectively.

The expansion is constructed under the assumption that zero is not an eigenvalue of the operator  $\mathcal{L}$  acting in the space of small-scale periodic solenoidal vector fields with vanishing mean. (By “small-scale” we understand “depending only on the fast variables”.)

The decomposition of the gradient  $\nabla = \nabla_{\mathbf{x}} + \epsilon \nabla_{\mathbf{y}}$ , applied to the solenoidality condition, expanded in powers of  $\epsilon$  and separated into mean and fluctuating part, gives

$$\nabla_{\mathbf{y}} \cdot \mathbf{H}_n = 0, \quad (\text{A.2})$$

$$\nabla_{\mathbf{x}} \cdot \mathbf{G}_n + \nabla_{\mathbf{y}} \cdot \mathbf{G}_{n-1} = 0 \quad (\text{A.3})$$

for all  $n \geq 0$ . ( $\mathbf{H}_n = \mathbf{G}_n \equiv 0$  is assumed for all  $n < 0$ .)

Substituting the expansions and the decomposition of the gradient into (A.1), we obtain:

$$\sum_{n=0}^{\infty} \left[ \mathcal{L} \mathbf{G}_n + \eta \left( 2(\nabla_{\mathbf{x}} \cdot \nabla_{\mathbf{y}}) \mathbf{G}_{n-1} + \nabla_{\mathbf{y}}^2 (\mathbf{H}_{n-2} + \mathbf{G}_{n-2}) \right) + \nabla_{\mathbf{x}} \times (\mathbf{v} \times \mathbf{H}_n) + \nabla_{\mathbf{y}} \times (\mathbf{v} \times (\mathbf{H}_{n-1} + \mathbf{G}_{n-1})) - \sum_{m=0}^n \lambda_{n-m} (\mathbf{H}_m + \mathbf{G}_m) \right] \epsilon^n = 0. \quad (\text{A.4})$$

We proceed by successively equating to zero the mean and the fluctuating part of each term of this series. In our context, averaging is equivalent to obtaining the solvability condition for a partial differential equation in fast variables.

*i.* Transform the leading ( $n = 0$ ) term of (A.4) using vector algebra identities and (4):

$$\mathcal{L} \mathbf{G}_0 + (\mathbf{H}_0 \cdot \nabla_{\mathbf{x}}) \mathbf{v} = \lambda_0 (\mathbf{H}_0 + \mathbf{G}_0). \quad (\text{A.5})$$

Averaging of this equation yields  $\lambda_0 = 0$ . Then the solution of (A.5) can be expressed as

$$\mathbf{G}_0 = \sum_{k=1}^3 \mathbf{S}_k(\mathbf{x}) H_0^k(\mathbf{y}), \quad (\text{A.6})$$

where the vector fields  $\mathbf{S}_k$  are the solutions of the first auxiliary problem (11); the solutions exist since it is assumed that the kernel of  $\mathcal{L}$  is empty. (The first and second auxiliary equations were stated in Section 2.)

By taking the divergence of the first auxiliary equation (11), one obtains  $\nabla_{\mathbf{x}} \cdot \mathbf{S}_k = 0$ . Since the velocity is parity-invariant, the domain of  $\mathcal{L}$  is a direct sum of two invariant subspaces, one of which is comprised of parity-invariant vector fields (i.e.  $\mathbf{f}(\mathbf{x}) = -\mathbf{f}(-\mathbf{x})$ ), and the second – of the parity-antiinvariant ones ( $\mathbf{f}(\mathbf{x}) = \mathbf{f}(-\mathbf{x})$ ). Thus,  $\mathbf{S}$  is a parity-antiinvariant matrix:

$$\mathbf{S}_k(\mathbf{x}) = \mathbf{S}_k(-\mathbf{x}). \quad (\text{A.7})$$

*ii.* The  $\epsilon^1$  term of (A.4), after the use of (A.2), takes the form

$$\begin{aligned} & \mathcal{L} \mathbf{G}_1 + 2\eta(\nabla_{\mathbf{x}} \cdot \nabla_{\mathbf{y}}) \mathbf{G}_0 + (\mathbf{H}_1 \cdot \nabla_{\mathbf{x}}) \mathbf{v} + \nabla_{\mathbf{y}} \times (\mathbf{v} \times \mathbf{G}_0) \\ & - (\mathbf{v} \cdot \nabla_{\mathbf{y}}) \mathbf{H}_0 = \lambda_1 (\mathbf{H}_0 + \mathbf{G}_0). \end{aligned} \quad (\text{A.8})$$

Substituting (A.6) in (A.8) and averaging, we obtain

$$\nabla_{\mathbf{y}} \times (\langle \mathbf{v} \times \mathbf{S} \rangle \mathbf{H}_0) = \lambda_1 \mathbf{H}_0. \quad (\text{A.9})$$

So far, developments strictly followed those of Vishik (1987), but here the point of divergence is reached. Since  $\mathbf{v}$  is parity-invariant (5) and  $\mathbf{S}$  is parity-antiinvariant (A.7), we have  $\langle \mathbf{v} \times \mathbf{S} \rangle = 0$ , and therefore (A.9) implies  $\lambda_1 = 0$ . Upon inserting (A.6) into the fluctuating part of (A.8), we obtain

$$\mathcal{L}\mathbf{G}_1 = -(\mathbf{H}_1 \cdot \nabla_{\mathbf{x}})\mathbf{v} + \sum_{k=1}^3 \sum_{m=1}^3 \left( -2\eta \frac{\partial \mathbf{S}_k}{\partial x_m} + v^m (\mathbf{S}_k + \mathbf{e}_k) - \mathbf{v} S_k^m \right) \frac{\partial \mathbf{H}_0^k}{\partial y_m}, \quad (\text{A.10})$$

from which one finds

$$\mathbf{G}_1 = \sum_{k=1}^3 \mathbf{S}_k(\mathbf{x}) H_1^k(\mathbf{y}) + \sum_{k=1}^3 \sum_{m=1}^3 \mathbf{\Gamma}_{mk}(\mathbf{x}) \frac{\partial H_0^k}{\partial y_m}(\mathbf{y}). \quad (\text{A.11})$$

Here, the nine vector fields  $\mathbf{\Gamma}_{mk}$  are solutions to the second auxiliary equation (12). Note  $\mathbf{\Gamma}_{mk}(\mathbf{x}) = -\mathbf{\Gamma}_{mk}(-\mathbf{x})$  by the symmetry properties of  $\mathbf{v}$ ,  $\mathbf{S}_k$  and of the operator  $\mathcal{L}$ . By taking divergence of the second auxiliary equation one finds  $\nabla_{\mathbf{x}} \cdot \mathbf{\Gamma}_{mk} + \mathbf{S}_k^m = 0$ . Hence, for  $n = 1$  (A.3) is automatically satisfied.

*iii.* The  $\epsilon^2$  term of (A.4) takes the form

$$\begin{aligned} & \mathcal{L}\mathbf{G}_2 + \eta \left( 2(\nabla_{\mathbf{x}} \cdot \nabla_{\mathbf{y}})\mathbf{G}_1 + \nabla_{\mathbf{y}}^2(\mathbf{H}_0 + \mathbf{G}_0) \right) + (\mathbf{H}_2 \cdot \nabla_{\mathbf{x}})\mathbf{v} \\ & + \nabla_{\mathbf{y}} \times (\mathbf{v} \times \mathbf{G}_1) - (\mathbf{v} \cdot \nabla_{\mathbf{y}})\mathbf{H}_1 = \lambda_2(\mathbf{H}_0 + \mathbf{G}_0). \end{aligned} \quad (\text{A.12})$$

Upon substitution of (A.11), averaging produces the second-order equation

$$\overline{\mathcal{M}}\mathbf{H}_0 \equiv \eta \nabla_{\mathbf{y}}^2 \mathbf{H}_0 + \nabla_{\mathbf{y}} \times \sum_{k=1}^3 \sum_{m=1}^3 \langle \mathbf{v} \times \mathbf{\Gamma}_{mk} \rangle \frac{\partial H_0^k}{\partial y_m} = \lambda_2 \mathbf{H}_0,$$

which defines the eddy diffusivity operator. So, the leading terms of the expansions of the mean magnetic field,  $\mathbf{H}_0$ , and of the associated eigenvalue,  $\lambda_2$ , satisfy the eigenvalue equation for this operator. Its eigenvectors are Fourier harmonics:  $\mathbf{H}_0 = \mathbf{h} e^{i\mathbf{q} \cdot \mathbf{y}}$ , where  $\mathbf{h}$  and  $\mathbf{q}$  are constant vectors satisfying (14) and (15). Note that the fluctuating part of the leading term of the eigenmode,  $\mathbf{G}_0$ , is now completely determined by (A.6).



At this point our construction goes beyond that of Lanotte *et al.* (1999) and, in the spirit of Vishik (1987), we show how to extend the analysis to higher orders in  $\epsilon$ .

The fluctuating part of (A.12) reads

$$\begin{aligned} \mathcal{L}\mathbf{G}_2 = & -\eta \left( 2 \sum_{k=1}^3 \sum_{m=1}^3 \left( \frac{\partial \mathbf{S}_k}{\partial x_m} \frac{\partial H_1^k}{\partial y_m} + \sum_{l=1}^3 \frac{\partial \Gamma_{mk}}{\partial x_l} \frac{\partial^2 H_0^k}{\partial y_m \partial y_l} \right) + \nabla_{\mathbf{y}}^2 \mathbf{G}_0 \right) \\ & - (\mathbf{H}_2 \cdot \nabla_{\mathbf{x}}) \mathbf{v} + (\mathbf{v} \cdot \nabla_{\mathbf{y}}) \mathbf{H}_1 \\ & - \nabla_{\mathbf{y}} \times \left( \sum_{k=1}^3 (\mathbf{v} \times \mathbf{S}_k) H_1^k + \sum_{k=1}^3 \sum_{m=1}^3 \{ \mathbf{v} \times \Gamma_{mk} \} \frac{\partial H_0^k}{\partial y_m} \right) + \lambda_2 \mathbf{G}_0. \end{aligned} \quad (\text{A.13})$$

Here, only the terms involving  $\mathbf{H}_2$  and  $\partial H_1^k / \partial y_m$  are not yet determined. However, as one can immediately see,  $\mathbf{x}$ -dependent prefactors in front of these terms are identical to those, which are in (A.10) in front of  $\mathbf{H}_1$  and  $\partial H_0^k / \partial y_m$ , respectively. This implies a representation

$$\mathbf{G}_2 = \sum_{k=1}^3 \mathbf{S}_k(\mathbf{x}) H_2^k(\mathbf{y}) + \sum_{k=1}^3 \sum_{m=1}^3 \Gamma_{mk}(\mathbf{x}) \frac{\partial H_1^k}{\partial y_m}(\mathbf{y}) + \mathbf{Q}_2(\mathbf{x}, \mathbf{y}),$$

where the vector field  $\mathbf{Q}_2$  can be uniquely determined from

$$\begin{aligned} \mathcal{L}\mathbf{Q}_2 = & -\eta \left( 2 \sum_{k=1}^3 \sum_{m=1}^3 \sum_{l=1}^3 \frac{\partial \Gamma_{mk}}{\partial x_l} \frac{\partial^2 H_0^k}{\partial y_m \partial y_l} + \nabla_{\mathbf{y}}^2 \mathbf{G}_0 \right) \\ & - \nabla_{\mathbf{y}} \times \sum_{k=1}^3 \sum_{m=1}^3 \{ \mathbf{v} \times \Gamma_{mk} \} \frac{\partial H_0^k}{\partial y_m} + \lambda_2 \mathbf{G}_0. \end{aligned}$$

*iv.* As already stated,  $\lambda_2$  is one of the two eigenvalues of (14)-(15). In what follows we assume that the other eigenvalue,  $\lambda'_2$ , is distinct from  $\lambda_2$  and we denote by  $\mathbf{h}'$  the associated eigenvector.

Equations arising at higher orders in  $\epsilon$  are now solved recursively. Assume that all the equations up to order  $\epsilon^{N-1}$  have been solved, so that the following information has been obtained:

- vector fields  $\mathbf{H}_n$  and  $\mathbf{G}_n$  for all  $n < N - 2$ ;
- representations of  $\mathbf{G}_n$  of the form

$$\mathbf{G}_n = \sum_{k=1}^3 \mathbf{S}_k(\mathbf{x}) H_n^k(\mathbf{y}) + \sum_{k=1}^3 \sum_{m=1}^3 \Gamma_{mk}(\mathbf{x}) \frac{\partial H_{n-1}^k}{\partial y_m}(\mathbf{y}) + \mathbf{Q}_n(\mathbf{x}, \mathbf{y}) \quad (\text{A.14})$$

for  $n = N - 1$  and  $n = N - 2$  with known vector fields  $\mathbf{Q}_n$ ,  $\langle \mathbf{Q}_n \rangle = 0$ ;

- quantities  $\lambda_n$  for  $n < N$ .

Upon substitution of (A.14) for  $n = N - 1$  the average of the equation at order  $\epsilon^N$  becomes

$$(\overline{\mathcal{M}} - \lambda_2)\mathbf{H}_{N-2} - \lambda_N\mathbf{H}_0 = -\nabla_{\mathbf{y}} \times \langle \mathbf{v} \times \mathbf{Q}_{N-1} \rangle + \sum_{m=1}^{N-3} \lambda_{N-m}\mathbf{H}_m,$$

where the right-hand side at this stage is a known vector field. Projecting this equation out in the direction of  $\mathbf{H}_0$  one can uniquely determine  $\lambda_N$ . In the complementary invariant subspace the operator  $\overline{\mathcal{M}} - \lambda_2$  is invertible, and hence  $\mathbf{H}_{N-2}$  can be determined up to an arbitrary multiple of  $\mathbf{H}_0$ . This additive term can be neglected: one can demand that  $\mathbf{H}_{N-2}$  belong to the complementary subspace. This is a normalization condition related to the fact that eigenvectors can be multiplied by arbitrary (analytic) functions of  $\epsilon$ . As a result,  $\mathbf{G}_{N-2}$  is now determined by (A.14) with  $n = N - 2$ .

Upon use of (A.14) for  $n = N - 1$  the fluctuating part of the equation at order  $\epsilon^N$  becomes

$$\begin{aligned} \mathcal{L}\mathbf{G}_N = & -\eta \left( 2 \sum_{k=1}^3 \sum_{m=1}^3 \left( \frac{\partial \mathbf{S}_k}{\partial x_m} \frac{\partial H_{N-1}^k}{\partial y_m} + \sum_{l=1}^3 \frac{\partial \Gamma_{mk}}{\partial x_l} \frac{\partial^2 H_{N-2}^k}{\partial y_l \partial y_m} \right) \right. \\ & + 2(\nabla_{\mathbf{x}} \cdot \nabla_{\mathbf{y}})\mathbf{Q}_{N-1} + \nabla_{\mathbf{y}}^2 \mathbf{G}_{N-2} \Big) - (\mathbf{H}_N \cdot \nabla_{\mathbf{x}})\mathbf{v} + (\mathbf{v} \cdot \nabla_{\mathbf{y}})\mathbf{H}_{N-1} \\ & - \nabla_{\mathbf{y}} \times \left( \sum_{k=1}^3 (\mathbf{v} \times \mathbf{S}_k) H_{N-1}^k + \sum_{k=1}^3 \sum_{m=1}^3 \{ \mathbf{v} \times \Gamma_{mk} \} \frac{\partial H_{N-2}^k}{\partial y_m} + \{ \mathbf{v} \times \mathbf{Q}_{N-1} \} \right) \\ & + \sum_{m=0}^{N-2} \lambda_{N-m} \mathbf{G}_m. \end{aligned} \quad (\text{A.15})$$

Only the terms involving  $\mathbf{H}_N$  and derivatives of  $H_{N-1}^k$  are not yet determined. Like in (A.13),  $\mathbf{x}$ -dependent prefactors in front of these terms are identical to those in front of  $\mathbf{H}_1$  and derivatives of  $\mathbf{H}_0^k$  in (A.10), respectively. Hence, (A.15) yields a representation of the form (A.14) for  $\mathbf{G}_N$ . An equation for  $\mathbf{Q}_N$  can be obtained from (A.15) by replacing  $\mathbf{G}_N$  by  $\mathbf{Q}_N$  and omitting all terms involving  $\mathbf{H}_N$  and derivatives of  $\mathbf{H}_{N-1}$ .

Thus, a complete formal decomposition of magnetic modes and their eigenvalues has been constructed. A step-by-step analysis of the solution reveals that

$$\mathbf{H}_0 = \mathbf{h} e^{i\mathbf{q} \cdot \mathbf{y}}, \quad \mathbf{H}_n = \chi_n \mathbf{h}' e^{i\mathbf{q} \cdot \mathbf{y}} \quad \forall n > 0$$

(with suitable scalars  $\chi_n$ ) and

$$\mathbf{G}_n = \mathbf{g}_n(\mathbf{x})e^{i\mathbf{q}\cdot\mathbf{y}} \quad \forall n \geq 0; \quad (\text{A.16})$$

thus the expanded eigenmode admits a representation (1) in the form of a plane wave in the slow variable. (For this reason it was sufficient to demand, for constructions presented under heading *iv*, that the two eigenvalues  $\lambda_2$  and  $\lambda'_2$  of  $\overline{\mathcal{M}}$  be distinct in the subspace of solenoidal vector fields  $\mathbf{c}e^{i\mathbf{q}\cdot\mathbf{y}}$  with  $\mathbf{c} = \text{const}$ , instead of requiring that  $\overline{\mathcal{M}} - \lambda_2$  be invertible in the whole domain.) The plane-wave representation does not come as a surprise, since the domain of the magnetic induction operator  $\mathcal{M}$  splits into invariant subspaces, each comprised of vector fields of the form (1) and categorized by wavevectors  $\mathbf{q}$ .

If the homogenized operator  $\overline{\mathcal{M}}$  turns out to be elliptic, one can prove, following Vishik (1986, 1987), that any point  $\lambda_2$  of the spectrum of  $\overline{\mathcal{M}}$  is associated with an analytic branch (8) of eigenvalues of the original magnetic induction operator  $\mathcal{M}$ . The proof relies on the general perturbation theory for linear operators (Kato, 1980); it will not be presented here.

## B Strongly negative eddy diffusivities

In this Appendix we discuss a mechanism for appearance of negative eddy diffusivities with arbitrarily large magnitudes.

Let  $\mathbf{f}_p(\eta)$  denote the basis of small-scale  $2\pi$ -periodic magnetic modes with vanishing mean and  $\zeta_p(\eta)$  – the associated eigenvalues:

$$\mathcal{L}\mathbf{f}_p(\eta) = \zeta_p(\eta)\mathbf{f}_p(\eta), \quad |\mathbf{f}_p(\eta)| = 1, \quad \nabla \cdot \mathbf{f}_p(\eta) = 0$$

(assuming in this section, for the sake of simplicity, that  $\mathcal{L}$  is diagonalizable). Suppose that when molecular diffusivity  $\eta$  is decreased, small-scale magnetic fields with vanishing mean loose stability in such a way that the dominant eigenvalue of the magnetic induction operator  $\mathcal{L}$  passes through zero. Let  $\eta_c$  be the critical diffusivity:

$$\text{Re } \zeta_p(\eta) < 0 \quad \forall p, \quad \forall \eta < \eta_c; \quad \zeta_1(\eta_c) = 0.$$

Generically, the loss of stability occurs either in the proper subspace comprised of parity-invariant fields, or in that of parity-antiinvariant fields, implying two possible variants of the mechanism.

Suppose small-scale parity-invariant magnetic fields are the first to loose stability. Solutions  $\mathbf{S}(\eta)$  to the first auxiliary problem (11) continuously depend on  $\eta$  for  $\eta < \eta_c$ . The second auxiliary problem (12) can be reexpressed as

$$\sum_p \zeta_p(\eta) \gamma_{mk,p}(\eta) \mathbf{f}_p(\eta) = \sum_p \kappa_{mk,p}(\eta) \mathbf{f}_p(\eta), \quad (\text{B.1})$$

where

$$-2\eta \frac{\partial \mathbf{S}_k(\eta)}{\partial x_m} + v^m (\mathbf{S}_k(\eta) + \mathbf{e}_k) - \mathbf{v} S_k^m(\eta) = \sum_p \kappa_{mk,p}(\eta) \mathbf{f}_p(\eta)$$

and

$$\mathbf{\Gamma}_{mk}(\eta) = \sum_p \gamma_{mk,p}(\eta) \mathbf{f}_p(\eta)$$

are decompositions of the r.h.s. of (12) and of  $\mathbf{\Gamma}_{mk}(\eta)$  in the basis of magnetic modes; summation over all parity-invariant eigenvectors is assumed in the two sums. From (B.1),  $\gamma_{mk,p}(\eta) = \kappa_{mk,p}(\eta)/\zeta_p(\eta)$ . Since generically the coefficients  $\kappa_{mk,1}(\eta_c)$  do not vanish, we have in the limit  $\eta \rightarrow \eta_c$

$$\mathbf{\Gamma}_{mk}(\eta) \approx \frac{\kappa_{mk,1}(\eta_c)}{\zeta_1(\eta)} \mathbf{f}_1(\eta_c) \rightarrow \infty.$$

Then the equation (14) for the eigenvalue  $\lambda_2$  asymptotically reduces to

$$\frac{\mathbf{A}(\mathbf{q})}{\zeta_1(\eta)} \sum_{k=1}^3 \sum_{m=1}^3 \kappa_{mk,1}(\eta_c) h^k q^m = -\lambda_2 \mathbf{h}, \quad (\text{B.2})$$

where  $\mathbf{A}(\mathbf{q}) \equiv \mathbf{q} \times \langle \mathbf{v} \times \mathbf{f}_1(\eta_c) \rangle$ . Equations (B.2) and (15) yield two eigenvalues. It is easily checked that one of them, denoted  $\lambda'_2$ , vanishes and thus is of no interest for us; the associated eigenvector  $\mathbf{h}'$  is orthogonal to the wavevector  $\mathbf{q}$  and satisfies

$$\sum_{k=1}^3 \sum_{m=1}^3 \kappa_{mk,1}(\eta_c) h^k q^m = 0.$$

The second eigenvalue is

$$\lambda_2 = -\frac{a(\mathbf{q})}{\zeta_1(\eta)}, \quad a(\mathbf{q}) \equiv \sum_{k=1}^3 \sum_{m=1}^3 \kappa_{mk,1}(\eta_c) A^k(\mathbf{q}) q^m,$$

the associated eigenvector being  $\mathbf{h} = \mathbf{A}(\mathbf{q})$  (we consider a generic case, where  $\mathbf{A}$  does not vanish). Therefore, if  $\hat{a} \equiv \max_{|\mathbf{q}|=1} a(\mathbf{q}) > 0$ , then, in the limit  $\eta \rightarrow \eta_c$ , the minimum magnetic eddy diffusivity becomes arbitrarily large negative:

$$\eta_{\text{eddy}} \approx \frac{\hat{a}}{\zeta_1(\eta)} \rightarrow -\infty.$$

Alternatively, suppose now that the loss of stability occurs in the subspace of small-scale parity-antiinvariant magnetic fields. Then the mechanism is similar. In this case already the solutions  $\mathbf{S}(\eta)$  to the first auxiliary problem (11) tend to infinity. Indeed, (11) can be represented as

$$\sum_p \zeta_p(\eta) s_{k,p}(\eta) \mathbf{f}_p(\eta) = \sum_p \rho_{k,p}(\eta) \mathbf{f}_p(\eta),$$

where

$$-\frac{\partial \mathbf{v}}{\partial x_k} = \sum_p \rho_{k,p}(\eta) \mathbf{f}_p(\eta)$$

and

$$\mathbf{S}_k(\eta) = \sum_p s_{k,p}(\eta) \mathbf{f}_p(\eta)$$

are decompositions of the r.h.s. of the first auxiliary problem (11) and of  $\mathbf{S}_k(\eta)$  in the basis of magnetic modes; summation over parity-antiinvariant eigenvectors is assumed in both sums. Thus,  $s_{k,p}(\eta) = \rho_{k,p}(\eta)/\zeta_p(\eta)$ . Since generically  $\rho_{k,1}(\eta_c) \neq 0$ , we have in the limit  $\eta \rightarrow \eta_c$

$$\mathbf{S}_k(\eta) \approx \frac{\rho_{k,1}(\eta_c)}{\zeta_1(\eta)} \mathbf{f}_1(\eta_c) \rightarrow \infty.$$

Let  $\gamma_m$  denote the solution to

$$\mathcal{L}\gamma_m = -2\eta_c \frac{\partial \mathbf{f}_1(\eta_c)}{\partial x_m} + v^m \mathbf{f}_1(\eta_c) - \mathbf{v} f_1^m(\eta_c).$$

Then

$$\mathbf{\Gamma}_{mk}(\eta) \approx \frac{\rho_{k,1}(\eta_c)}{\zeta_1(\eta)} \gamma_m,$$

and (14) asymptotically reduces to

$$\frac{\mathbf{B}(\mathbf{q})}{\zeta_1(\eta)} \sum_{k=1}^3 \rho_{k,1}(\eta_c) h^k = -\lambda_2 \mathbf{h}, \quad (\text{B.3})$$

where

$$\mathbf{B}(\mathbf{q}) \equiv \sum_{m=1}^3 q^m \mathbf{q} \times \langle \mathbf{v} \times \boldsymbol{\gamma}_m \rangle.$$

Equations (B.3) and (15) yield two eigenvalues. Again, one can easily check that one of them,  $\lambda'_2$ , vanishes; the associated eigenvector  $\mathbf{h}'$  is orthogonal to  $\mathbf{q}$  and satisfies

$$\sum_{k=1}^3 \rho_{k,1}(\eta_h) h''^k = 0.$$

The second is

$$\lambda_2 = -\frac{b(\mathbf{q})}{\zeta_1(\eta)}, \quad b(\mathbf{q}) \equiv \sum_{k=1}^3 \rho_{k,1}(\eta_c) B^k(\mathbf{q}),$$

with the associated vector  $\mathbf{h} = \mathbf{B}(\mathbf{q})$  (in the generic case  $\mathbf{B} \neq 0$ ). Therefore, if  $\hat{b} \equiv \max_{|\mathbf{q}|=1} b(\mathbf{q}) > 0$ , when  $\eta \rightarrow \eta_c$  the minimum magnetic eddy diffusivity becomes again arbitrarily large negative:

$$\eta_{\text{eddy}} \approx \frac{\hat{b}}{\zeta_1(\eta)} \rightarrow -\infty.$$

## C Chebyshev iterative methods for numerical solution of systems of equations

We discuss here three Chebyshev iterative methods suitable for large systems of linear or non-linear equations. They employ extremal properties of Chebyshev polynomials and their roots. The first method (*Ch1*), discussed in Subsection C.1, is applicable to problems with negative-definite self-adjoint Jacobians. An extension (*Ch1a*), discussed in Subsection C.2, is an upgrade of *Ch1*, which eliminates these restrictions. The second method (*Ch2*), discussed in Subsection C.3, is designed for discretizations of elliptic differential equations, such as the auxiliary problems (11) and (12). *Ch1* and *Ch1a* were introduced by Podvigina and Zheligovsky (1997) and *Ch2* is presented in detail in Zheligovsky (2001). For general background on Chebyshev iterative methods, see Axelsson (1996).

## C.1 The basic method: restricted case (*Ch1*)

We consider numerical solution of a system of equations

$$\mathbf{F}(\mathbf{z}) = 0, \quad (\text{C.1})$$

where  $\mathbf{F} : \mathbf{C}^N \rightarrow \mathbf{C}^N$  is smooth and the number of equations,  $N$ , is large.

Let  $\mathbf{z} = \mathbf{Z}$  be a solution to (C.1). We first consider the case, where the Jacobian matrix  $\mathbf{F}'(\mathbf{Z})$  is diagonalizable and its spectrum is (real and) negative. Then the solution can be computed by iterations

$$\mathbf{z}_1 = \mathbf{z}_0 + h\mathbf{F}(\mathbf{z}_0), \quad (\text{C.2})$$

$$\mathbf{z}_{k+1} = \gamma_k (\mathbf{z}_k + h\mathbf{F}(\mathbf{z}_k)) + (1 - \gamma_k)\mathbf{z}_{k-1}, \quad k > 0, \quad (\text{C.3})$$

provided  $\mathbf{z}_0$  is chosen in the basin of attraction of  $\mathbf{Z}$ . Here

$$h \equiv \frac{2}{\Lambda + \lambda}, \quad \gamma_k \equiv 2\mu \frac{T_k(\mu)}{T_{k+1}(\mu)}, \quad \mu \equiv \frac{\Lambda + \lambda}{\Lambda - \lambda}, \quad (\text{C.4})$$

where  $0 \leq \lambda < \Lambda$  for any  $\Lambda \geq |\mathbf{F}'(\mathbf{Z})|$  (the optimal value  $\Lambda = |\mathbf{F}'(\mathbf{Z})|$  is usually unknown), and where the  $T_k$ 's are Chebyshev polynomials of the first kind. The  $\gamma_k$ 's can be evaluated recursively:

$$\gamma_0 = 2; \quad \gamma_k = \frac{4\mu^2}{4\mu^2 - \gamma_{k-1}}, \quad k > 0. \quad (\text{C.5})$$

Consider how the discrepancy vectors  $\boldsymbol{\zeta}_k \equiv \mathbf{z}_k - \mathbf{Z}$  evolve in the course of iterations (C.2)-(C.5). Introduce the eigenvalues  $\eta_i$  of  $\mathbf{F}'(\mathbf{Z})$  (here,  $0 > \eta_i \geq -\Lambda$ ) and the associated eigenvectors  $\{\mathbf{e}_i\}$ , and decompose the initial discrepancy in this basis:

$$\boldsymbol{\zeta}_0 = \sum_{i=1}^N c^i \mathbf{e}_i.$$

It is then easily shown that

$$\boldsymbol{\zeta}_k = \sum_{i=1}^N \frac{T_k(\mu(1 + h\eta_i))}{T_k(\mu)} c^i \mathbf{e}_i + o(|\boldsymbol{\zeta}_0|), \quad k \geq 0$$

(the  $o(|\boldsymbol{\zeta}_0|)$  correction does not appear if the mapping  $\mathbf{F}$  is linear).

At this point, the standard strategy is to use the least deviation principle for Chebyshev polynomials: the iterative process (C.2)-(C.5) with  $\lambda > 0$  ensures maximum uniform decay of the discrepancy vector component in the proper subspace of  $\mathbf{F}'(\mathbf{Z})$  associated with the part of the spectrum in the interval  $-\lambda \geq \eta_i \geq -\Lambda$ . The alternative procedure used by Podvigina and Zheligovsky (1997) relies, in addition, on the extremal property of the largest root of a Chebyshev polynomial: for  $\lambda = 0$ , the iterative process gives optimal reduction of the discrepancy vector component in the proper subspace of  $\mathbf{F}'(\mathbf{Z})$  associated with eigenvalues  $\eta_i$  closest to zero. Therefore, a suitable algorithm, called here *Ch1*, consists of a succession of iterative sequences (C.2)-(C.5) with  $\lambda > 0$  and  $\lambda = 0$ .

As usually, lowering of the condition number of the system allows to improve efficiency of the algorithm. If, in addition,  $\mathbf{F}'(\mathbf{Z})$  is self-adjoint, such lowering can be achieved by replacing (C.1) with an equivalent system

$$\hat{\mathbf{F}}(\mathbf{z}) = 0,$$

where

$$\hat{\mathbf{F}}(\mathbf{z}) \equiv \mathbf{P}(\mathbf{z}) \cdot \mathbf{F}(\mathbf{z}), \quad (\text{C.6})$$

$\mathbf{P}(\mathbf{z})$  being a self-adjoint and positive-definite linear preconditioning operator. It may be checked that for such a  $\mathbf{P}(\mathbf{z})$  the mapping  $\hat{\mathbf{F}}$  has the required properties stated at the beginning of this subsection.

## C.2 An extension of *Ch1*: general case (*Ch1a*)

In the case of an arbitrary smooth mapping  $\mathbf{F}$ , to which we turn now, a modified system

$$\tilde{\mathbf{F}}(\mathbf{z}) = 0$$

can be considered, where

$$\tilde{\mathbf{F}}(\mathbf{z}) \equiv -\mathbf{P}_1(\mathbf{z}) \cdot (\mathbf{F}'(\mathbf{z}))^* \cdot \mathbf{P}_2(\mathbf{z}) \cdot \mathbf{F}(\mathbf{z}), \quad (\text{C.7})$$

$\mathbf{P}_i$  ( $i = 1, 2$ ) being arbitrary positive definite self-adjoint operators and  $\mathbf{M}^* = \overline{\mathbf{M}}^t$  being the operator adjoint to  $\mathbf{M}$ . The method discussed above can be applied for the solution of the modified system, since  $\tilde{\mathbf{F}}'(\mathbf{Z})$  has all the required properties.



Termination of individual sequences and selection of values of  $\lambda$  in successive sequences is controlled by the following rules:

1. In the first iterative sequence  $\lambda = \lambda_1$ .
2. In any of the following iterative sequences  $\lambda = 0$ , unless  $\lambda$  was zero in the previous sequence and that sequence was short (i.e. it consisted of less than  $\left\lceil \pi \sqrt{\frac{\Lambda}{8\lambda_1}} + 1 \right\rceil$  iterations, where  $\lceil \cdot \rceil$  denotes the integer part of a number), in which case in the next sequence  $\lambda = \lambda_1$ .
3. An iterative sequence with  $\lambda = \lambda_1$  can be terminated only after a prescribed number of iterations have been performed.
4. In an iterative sequence with  $\lambda = 0$  the errors  $|\mathbf{F}(\mathbf{z}_k)|$  can initially grow monotonically, if the respective errors  $|\tilde{\mathbf{F}}(\mathbf{z}_k)|$  decrease monotonically. (An increase of  $|\mathbf{F}(\mathbf{z}_k)|$  at the first iteration indicates that  $\Lambda$  is underestimated.)
5. After the initial phase allowed by rules 3 or 4 is completed, an iterative sequence is terminated if both discrepancy reduction rate values,  $\frac{1}{k} \ln \frac{|\mathbf{F}(\mathbf{z}_0)|}{|\mathbf{F}(\mathbf{z}_k)|}$  and  $\frac{1}{k} \ln \frac{|\tilde{\mathbf{F}}(\mathbf{z}_0)|}{|\tilde{\mathbf{F}}(\mathbf{z}_k)|}$ , are smaller than at the previous iteration.
6. Either the last or the next to last iterate is accepted as the output of a sequence – specifically, the one, for which the error  $|\mathbf{F}(\mathbf{z}_k)|$  is smaller.

With these rules, the behavior of the algorithm proved insensitive to the particular choice of  $\lambda_1$  in the interval  $0.1\Lambda \leq \lambda_1 \leq 0.5\Lambda$ .

Only trivial changes to this set of rules are required to make it applicable to *Ch1*.

*Ch1a* proved robust and efficient, e.g. in computation of steady states of the Navier–Stokes equation (Podvigina, 1999a,b). However, the use of (C.7) may be potentially disadvantageous, because:

- The presence of the adjoint to  $\mathbf{F}'(\mathbf{z})$  leads to an increase in the condition number, which may not be completely neutralized by the preconditioning operators  $\mathbf{P}_1$  and  $\mathbf{P}_2$ .
- Computation of  $\tilde{\mathbf{F}}$  involves more operations (and hence larger codes) than that of the original mapping  $\mathbf{F}$ .
- Spurious roots may appear.

### C.3 An adaptation of *Ch1* to elliptic PDE's (*Ch2*)

We present here an alternative to *Ch1a*, better suited to problems arising from discretization of elliptic partial differential equations, when they involve not just leading-order elliptic operators (such as the Laplacian), but also

lower-order non-self-adjoint perturbations. We do not attempt to present this method in full generality (see Zheligovsky, 2001). In what follows the resolution of the discretization, assumed to be large, is the control parameter, which we denote by  $R$ .

Construction of the modified mapping (C.7) can be avoided under the conditions, that the basic mapping  $\mathbf{F}$  can be split:

$$\mathbf{F}(\mathbf{z}) = \mathbf{D}(\mathbf{z}) + \mathbf{A}(\mathbf{z}) \quad (\text{C.8})$$

and if a linear invertible preconditioning operator  $\mathbf{P}$  can be selected, such that:

1. All eigenvalues  $\sigma_i$  of the linear operator  $\mathcal{D} \equiv \mathbf{P} \cdot \mathbf{D}'(\mathbf{Z})$  are negative. (If  $\mathbf{P}$  is a self-adjoint positive-definite operator and  $\mathbf{D}'(\mathbf{Z})$  is a self-adjoint negative-definite operator, this condition is automatically verified.)
2. The ratio  $\delta \equiv |\mathcal{A}|/\Lambda$  is small for large  $R$ . Here  $\mathcal{A} \equiv \mathbf{P} \cdot \mathbf{A}'(\mathbf{Z})$ , and  $\Lambda$  is a “tight” upper bound for the spectral radius of  $\mathcal{D}$ , i.e. a bound, which stays of the order of the spectral radius for large resolutions.
3. The operators  $\mathcal{D}$  and  $\mathcal{A}$  nearly commute:  $|\mathcal{D}\mathcal{A} - \mathcal{A}\mathcal{D}| = o(|\mathcal{D}\mathcal{A}|)$ . (Note, that this condition is not that restrictive: it holds automatically in the absence of preconditioning, if  $\mathcal{D}$  is for example the Laplacian.)

A decomposition (C.8) arises naturally if the problem (C.1) is a discretization of a dissipative partial differential equation: then the mapping  $\mathbf{D}$  can be identified with the higher-order elliptic part of the equation, and  $\mathbf{A}$  – with the remaining terms. Auxiliary problems (11) and (12) arising from the two-scale expansion fall into this class.

Under the conditions stated above a modification of the method discussed in Subsection C.1, named *Ch2*, can be applied. Solution proceeds by a succession of Chebyshev iterative sequences (C.3)-(C.5), but the first iteration in all sequences is made differently. Suppose a termination condition (for example, the one considered in the previous subsection) for a Chebyshev sequence number  $n - 1$  is verified for the first time in this sequence for the iterate  $\mathbf{z}_K^{n-1}$  (we then call  $K$  the termination signal number). Then the sequence is continued by  $M$  further iterations, and we start the next sequence, by selecting

$$\mathbf{z}_0^n = \mathbf{z}_K^{n-1}; \quad \mathbf{z}_1^n = \mathbf{z}_K^{n-1} + h \left( \mathcal{D}(\mathbf{z}_K^{n-1}) + \mathcal{A}(\mathbf{z}_{K+M}^{n-1}) \right).$$

Subsequent iterations are defined as in (C.3):

$$\mathbf{z}_{k+1}^n = \gamma_k \left( \mathbf{z}_k^n + h \hat{\mathbf{F}}(\mathbf{z}_k^n) \right) + (1 - \gamma_k) \mathbf{z}_{k-1}^n, \quad k > 0.$$

(The quantities  $h$ ,  $\mu$  and  $\gamma_k$  were defined by (C.4)-(C.5) and  $\hat{\mathbf{F}}$  – by (C.6).)

In this iterative process, errors behave in the following way. Discrepancy vectors  $\boldsymbol{\zeta}_k^n \equiv \mathbf{z}_k^n - \mathbf{Z}$  can be represented in terms of Chebyshev polynomials of the first ( $T_k$ ) and of the second ( $U_k$ ) kind:

$$\boldsymbol{\zeta}_k^n = \frac{1}{T_k(\mu)} (T_k(\mathcal{Q}) \mathbf{a}^n + U_k(\mathcal{Q}) \mathbf{b}^n) + o(|\boldsymbol{\zeta}_0^n|),$$

where  $\mathcal{Q} \equiv \mu(\mathbf{I} + h(\mathcal{D} + \mathcal{A}))$ ,  $\mathbf{I}$  is the identity operator, and vectors  $\mathbf{a}^n$  and  $\mathbf{b}^n$ , which we call the basic error vectors, can be determined from  $\boldsymbol{\zeta}_0^n$  and  $\boldsymbol{\zeta}_1^n$ . (The terms  $o(|\boldsymbol{\zeta}_k^n|)$  do not emerge if the mapping  $\mathbf{F}$  is linear; in what follows they are neglected.)

Now, suppose that for the  $(n - 2)$ -nd sequence the termination signal number  $K$  was the same as for the  $(n - 1)$ -st iteration (in computations, successive Chebyshev sequences often do have equal lengths). Then it can be shown that

- $|\mathbf{b}^n| = O(\delta |\mathbf{a}^{n-1}|)$  and thus convergence of  $\mathbf{b}^n$  is slaved to convergence of  $\mathbf{a}^n$ .

- Within the succession of iterative sequences, the basic error vectors evolve as follows:

$$\mathbf{a}^n = \sum_{i=1}^N \frac{a_i^{n-1}}{T_K(\mu)} (T_K(\xi_i) \mathbf{e}_i + h \mu f_i T'_K(\xi_i) \mathcal{A} \mathbf{e}_i) + o(\delta |\mathbf{a}^{n-1}|), \quad (\text{C.9})$$

where

$$f_i \equiv 1 + \frac{1}{K} \left( \frac{T_K(\mu)}{T_{K+M}(\mu)} \frac{T_{K+M}(\xi_i)}{T_K(\xi_i)} - 1 \right),$$

$\xi_i \equiv \mu(1 + h\sigma_i)$ ,  $\sigma_i$  being eigenvalues of  $\mathcal{D}$ , and the coefficients  $a_i^{n-1}$  can be found from the decomposition of  $\mathbf{a}^{n-1}$  in the basis of eigenvectors  $\mathbf{e}_i$  of  $\mathcal{D}$ :

$$\mathbf{a}^{n-1} = \sum_{i=1}^N a_i^{n-1} \mathbf{e}_i.$$

Thus, reduction of the basic error vectors  $\mathbf{a}^n$  is predominantly controlled by  $\mathcal{D}$  (note that  $h|\mathcal{A}| = O(\delta)$ ). The standard first Chebyshev iteration (C.2)

is recovered when one sets  $M = 0$  and hence  $f_i = 1$ . It may be shown that our procedure leads to factors  $0 < f_i < 1$ , and thus to enhanced convergence, for eigenvalues sufficiently small in absolute value (provided  $\lambda = 0$  or  $\lambda$  is small). For the other eigenvalues good convergence is ensured as usually. (Actually, because of the presence of the non-self-adjoint perturbation  $\mathcal{A}$ , fast convergence is guaranteed only for eigenvalues large in absolute value; for those of intermediate magnitude slowdown might occur, but has not been observed in any of the cases we studied.) Of course, these convergence arguments hold only in so far as the resolution  $R$  is high enough and thus  $\delta$  is small enough to justify keeping only the leading terms in (C.9).

In the application of the generalized Chebyshev method to the auxiliary problems (11) and (12), we take  $\mathbf{D} = \eta \nabla^2$  (more precisely,  $D$  is the Fourier–Galerkin discretization of this operator). We select the preconditioning operator  $\mathbf{P} = (-\mathbf{D})^{-q}$  for some  $0 < q < 1$  by analogy with Podvigina and Zheligovsky (1997) and Podvigina (1999a,b). Then  $\mathcal{D} = -(-\mathbf{D})^{1-q}$  is a pseudodifferential operator of order  $2 - 2q$ , and  $\mathcal{A}$  – of order  $1 - 2q$ . Hence, Condition 2 is inherited from the non-discretized versions of the operators for  $q < 1$ . Condition 3 is satisfied for  $q < 3/4$ . Indeed, in the commutator  $\mathcal{D}\mathcal{A} - \mathcal{A}\mathcal{D}$  the leading symbols cancel out and therefore its order is by 1 less than the order of each of the operators  $\mathcal{D}\mathcal{A}$  and  $\mathcal{A}\mathcal{D}$ ; thus  $|\mathcal{D}\mathcal{A} - \mathcal{A}\mathcal{D}| = O(R^{\max(0, 2-4q)})$ ,  $|\mathcal{D}\mathcal{A}| = O(R^{\max(0, 3-4q)})$ , where  $R$  is the maximum wavenumber of the Fourier harmonics, retained in the abridged series, this completing the argument. Since Condition 3 is also trivially satisfied for  $q = 1$ , it is natural to consider the larger interval  $0 \leq q \leq 1$ , and we find the convergence to be the best for  $q = 3/4$ . When applied to (11) and (12), *Ch2* proved superior to *Ch1a*.

## References

- O. Axelsson, *Iterative solution methods*. Cambridge Univ. Press (1996).
- Bensoussan A., Lions J.-L. and Papanicolaou G. *Asymptotic Analysis for Periodic Structures*, North Holland (1978).
- Busse F.H. “Homogeneous dynamos in planetary cores and in the laboratory”, *Ann. Rev. Fluid Mech.* **32**, 383–408 (2000).
- Dubrulle B. and Frisch U. “Eddy viscosity of parity-invariant flow”, *Phys. Rev. A* **43**, 5355–5364 (1991).
- Fauve S. *Recherche expérimentale sur l’effet dynamo* (in French), Laboratoire de Physique Statistique (CNRS, UMR 8550), Ecole Normale Supérieure, Paris, France, 5 pp. (1999).
- Frisch U. *Turbulence. The legacy of A.N. Kolmogorov*, Cambridge Univ. Press (1995).
- Frisch U., Zhen Su She and Thual O. “Viscoelastic behaviour of cellular solutions to the Kuramoto-Sivashinsky model”, *J. Fluid Mech.* **168**, 221–240 (1986).
- Gailitis A., Lielausis O.A., Dement’ev S., Platacis E., Cifersons A., Gerbeth G., Gundrum T., Stefani F., Christen M., Haïel H. and Will G. “Detection of a flow induced magnetic field eigenmode in the Riga dynamo facility”, *Phys. Rev. Lett.* **84**, 4365–4368 (2000).
- Galanti B., Sulem P.L. and Pouquet A. “Linear and non-linear dynamos associated with ABC flows”, *Geophys. Astrophys. Fluid Dynamics* **66**, 183–208 (1992).
- Gama S., Vergassola M. and Frisch U. “Negative eddy viscosity in isotropically forced two-dimensional flow: linear and nonlinear dynamics”, *J. Fluid Mech.* **260**, 95–126 (1994).
- Kato T. *Perturbation theory for linear operators*, Springer-Verlag, Berlin, Heidelberg, New York (1980).

- Kozlov S.M. “Averaging of differential operators with almost periodic fast oscillating coefficients” (in Russian), *Matematicheskii sbornik* **107** N2, 199–217 (1978).
- Kraichnan R.H., “Diffusion of weak magnetic fields by isotropic turbulence,” *J. Fluid Mech.* **75**, 657–676 (1976).
- Krause F. and Rädler K.-H. *Mean-field Magnetohydrodynamics and Dynamo Theory*, Academic-Verlag, Berlin (1980).
- Lanotte A., Noullez A., Vergassola M. and Wirth A. “Large-scale dynamo by negative magnetic eddy diffusivities”, *Geophys. Astrophys. Fluid Dynamics* **91**, 131–146 (1999).
- Nore C., Brachet M.E., Politano H., Pouquet A. “Dynamo action in the Taylor–Green vortex near threshold”, *Phys. Plasmas* **4**, 1–3 (1997).
- Podvigina O.M. “Spatially-periodic steady solutions to the three-dimensional Navier-Stokes equation with the ABC-force”, *Physica D* **128**, 250–272 (1999a).
- Podvigina O.M. *Evolutionary and steady solutions to the Navier-Stokes equation with the ABC forcing* (in Russian), Institute of Mechanics, Lomonosov Moscow State University (1999b).
- Podvigina O.M. and Zheligovsky V.A. “An optimized iterative method for numerical solution of large systems of equations based on the extremal property of zeroes of Chebyshev polynomials”, *J. Sci. Computing* **12**, 433–464 (1997).
- Press W.H., Teukolsky S.A., Vetterling W.T. and Flannery B.P. *Numerical Recipes*, Cambridge Univ. Press (1992).
- Roberts G.O., “Dynamo action of fluid motions with two-dimensional periodicity,” *Phil. Trans. R. Soc. Lond.* **A271**, 411–454 (1972).
- Steenbeck M., Krause F., Rädler K.-H. “A calculation of the mean electromotive force in an electrically conducting fluid in turbulent motion, under the influence of Coriolis forces”, *Z. Naturforsch* **21a**, 369–376 (1966).
- Stieglitz R. and Müller U. “An experimental demonstration of a homogeneous two scale dynamo”, *Proceed. NATO ARW “Dynamo and dynamics*,

*a mathematical challenge*”, August 21-26, 2000, Institut d’Études Scientifiques de Cargèse, to appear (2000).

Vishik M.M. “Periodic dynamo. I” (in Russian), in *Mathematical Methods of Seismology and Geodynamics* (*Comput. Seism.* iss. **19**), Nauka, Moscow, 186–215 (1986).

Vishik M.M. “Periodic dynamo. II” (in Russian), in *Numerical Modeling and Analysis of Geophysical Processes* (*Comput. Seism.* iss. **20**), Nauka, Moscow, 12–22 (1987).

Wirth A., Gama S. and Frisch U. “Eddy viscosity of three-dimensional flow”, *J. Fluid Mech.* **288**, 249–264 (1995).

Zheligovsky V. “Numerical solution of the kinematic dynamo problem for Beltrami flows in a sphere”, *J. Sci. Computing* **8**, 41–68 (1993).

Zheligovsky V.A. “A Chebyshev iterative method with operator splitting for evaluation of roots of large systems of equations” (in Russian), accepted *Proc. International Workshop on Nonlinear Problems of hydrodynamic stability, Moscow, 2000*. Institute of Mechanics, Lomonosov Moscow State University, Moscow Univ. Press (2001). Also available at <http://www.obs-nice.fr/etc7/vlad.ps.gz>

Zhikov V.V., Kozlov S.M., Oleynik O.A. and Ha Tien Ngoan. “Averaging and  $G$ -convergence of differential operators” (in Russian), *Uspekhi Matematicheskikh Nauk* **34** N5, 63–133 (1979).